Multiple temperature scales of the periodic Anderson model: Slave boson approach

S. Burdin[1] and V. Zlatić[2]
[1]*Institut für Theoretische Physik, Universität zu Köln, Zülpicher Str. 77, 50937 Köln, Germany*
[2]*Institute of Physics, P.O. Box 304, 10001 Zagreb, Croatia*

(Received 28 November 2008; revised manuscript received 4 February 2009; published 31 March 2009)

The thermodynamic and transport properties of intermetallic compounds with Ce, Eu, and Yb ions are discussed using the periodic Anderson model with an infinite correlation between f electrons. At high temperatures, these systems exhibit typical features that can be understood in terms of a single-impurity Anderson or Kondo model with Kondo scale T_K. At low temperatures, one often finds a normal state governed by the Fermi liquid (FL) laws with characteristic energy scale T_0. The slave boson solution of the periodic model shows that T_0 and T_K depend not only on the degeneracy and the splitting of the f states, the number of c and f electrons, and their coupling but also on the shape of the conduction-electrons density of states (c DOS) in the vicinity of the chemical potential μ. The ratio T_0/T_K depends on the details of the band structure which makes the crossover between the high- and low-temperature regimes system dependent. We show that the c DOS with a sharp peak close to μ yields $T_0 \ll T_K$, which explains the "slow crossover" observed in $YbAl_3$ or $YbMgCu_4$. The c DOS with a minimum or a pseudogap close to μ yields $T_0 \gg T_K$; this leads to an abrupt transition between the high- and low-temperature regimes, as found in $YbInCu_4$-like systems. In the case of $CeCu_2Ge_2$ and $CeCu_2Si_2$, where $T_0 \simeq T_K$, we show that the pressure dependence of the T^2 coefficient of the electrical resistance, $A=\rho(T)/T^2$, and the residual resistance are driven by the change in the degeneracy of the f states. The FL laws obtained for $T \ll T_0$ explain the correlation between the specific-heat coefficient $\gamma=C_V/T$ and the thermopower slope $\alpha(T)/T$ or between γ and the resistivity coefficient A. The FL laws also show that the Kadowaki-Woods ratio, $R_{KW}=A/\gamma^2$, and the ratio $q=\lim_{\{T\to 0\}}\alpha/\gamma T$ assumes nonuniversal values due to different low-temperature degeneracies of various systems. The correlation effects can invalidate the Wiedemann-Franz law and lead to an enhancement of the thermoelectric figure of merit. They can also enhance (or reduce) the low-temperature response of the periodic Anderson model with respect to the predictions of a single-impurity model with the same high-temperature behavior as the periodic one.

DOI: 10.1103/PhysRevB.79.115139 PACS number(s): 71.27.+a, 71.10.Fd, 71.20.Eh

I. INTRODUCTION

Intermetallic compounds containing cerium, ytterbium, and europium ions exhibit a number of remarkable phenomena, such as the heavy fermion mass enhancement, valence fluctuations, huge thermopower, spin-charge separation, unconventional magnetism, and superconductivity, etc. Despite being studied for several decades, these systems are still attracting a considerable attention and are far from being understood. The initial focus was on dilute alloys with magnetic $3d$ and $4f$ impurities which shows qualitatively different behaviors at low and high temperatures. The high-temperature data indicate that the f states are localized and weakly coupled to conduction states. The susceptibility is of the Curie-Weiss form and entropy is large, as expected of nearly free f ions. At the same time, the logarithmic resistivity and large thermopower indicate that the conduction (c) electrons are weakly perturbed by the local moments (LMs). Such a behavior is explained by the perturbative solution of the Anderson or Kondo models, which yield the low-energy correlation functions as universal functions of reduced temperature T/T_K, where T_K is the Kondo temperature. The low-temperature data show that the susceptibility is Pauli like, the specific heat and entropy are linear in temperature, and transport coefficients are given by simple powers of reduced temperature T/T_K. Close to the ground state, the c and f states of opposite spin are tightly bound in a nonmagnetic singlet with fermionic excitation spectrum and an energy scale T_K. The overall behavior of dilute alloys with paramagnetic impurities is nearly the same when plotted on the T/T_K scale, even though the values of T_K can vary by orders of magnitude. Unlike the high-temperature data, neither the crossover nor the low-temperature behavior can be understood in terms of the perturbation theory which treats the conduction electrons and the local moments as separate entities. The fact that the low-temperature scale coincides with the high-temperature one and that the crossover from the weak- to the strong-coupling regime takes place around T_K indicates that these are the most prominent features of dilute Kondo systems.

The solution of the dilute alloy problem came after several decades of intensive work on the Kondo and the Anderson models. Early calculations considered the exchange scattering of conduction electrons with a constant density of states (c DOS) on spin-1/2 local moments. The solution was obtained by the variety of methods such as the perturbative scaling,[1] the numerical renormalization group,[2] the Fermi liquid theory,[3,4] and Bethe ansatz.[5] These results reveal that the effective coupling between the free fermions and degenerate local moments increases at low temperatures and diverges in the ground state, which explains the breakdown of the perturbation theory. However, the simple models cannot provide a quantitative description of dilute Kondo alloys; a realistic modeling has to take into account the details of the local states and the band structure of the host and consider additional scattering mechanisms. In Kondo systems with Ce and Yb ions, the splitting of the $4f$ states by the spin-orbit and the crystal-field (CF) effects can change the effective

degeneracy of the system, reduce the Kondo scale, and lead to the seemingly complicated features such as the multiple peaks in the resistivity or the sign change in the thermopower and the Hall effect. A nonconstant c DOS leads also to complicated low-temperature behaviors. Whithoff and Fradkin[6] found that the c DOS with a power-law singularity leads to a critical coupling J_c that separates different ground states. For $J>J_c$, the ground state is of the strong-coupling type, while for $J<J_c$ the renormalized coupling decreases with temperature and the "usual" Kondo screening of local moments does not occur.[7] Nevertheless, despite a conduction-electron pseudogap, it has been shown that Kondo-lattice screening can be more stable than in the single Kondo impurity case.[8]

The Kondo problem becomes much more difficult for stoichiometric compounds in which a magnetic ion is present in each unit cell. The high-temperature features can still be explained by an effective single-impurity model which takes into account additional splittings of the f states and/or the fact that c DOS can change rapidly in the vicinity of the chemical potential. The perturbation theory of such effective models provides a consistent picture of the high-temperature data: it yields the correct Kondo scale, explains the Curie-Weiss behavior of the susceptibility and the logarithmic decrease in the resistivity and thermopower, and accounts for the well-resolved CF excitations seen in neutron experiments. However, at sufficiently low temperatures, the scattering becomes coherent and one finds new features that cannot be explained by the single-impurity models. The onset of coherence is most clearly seen in the electrical resistivity which drops to very small values. It is also seen in the optical conductivity which shows the development of a low-frequency Drude peak and a small hybridization gap close to the chemical potential. At lowest temperatures, the Fermi liquid laws often emerge: the resistivity is quadratic and the thermopower is a linear function of temperature; the specific heat and the magnetic susceptibility are much enhanced, indicating a large effective electronic mass; the de Haas–van Alphen experiments show that f electrons contribute to the Fermi volume. The low-temperature ratios of various correlation functions, such as the Wilson ratio, χ/γ or the Kadowaki-Woods ratio A/γ^2, are close to the universal values. Here, γ and χ denote the $T\rightarrow 0$ limit of the specific-heat coefficient and the magnetic susceptibility and A is the coefficient of the T^2 term in the resistivity. The near universality of these ratios indicates that the ground-state properties depend on a single energy scale T_0. However, unlike in dilute alloys, this FL scale T_0 can be much different from T_K.

In this paper, we study the periodic systems with $4f$ ions and show that the relative magnitude of the Kondo and the FL scale depends on the shape of the unperturbed conduction states. For the Anderson lattice with an enhanced DOS around the chemical potential, we find $T_0 \ll T_K$, which explains the gradual transition between the coherent and the incoherent regimes (slow crossover) observed in $YbAl_3$.[9] A pseudogap or a reduced c DOS close to the chemical potential yields $T_K \ll T_0$, which explains the abrupt valence-change transition observed in Yb- and Eu-based intermetallic compounds such as $YbInCu_4$,[10] $EuNi_2(Si_{1-x}Ge_x)_2$,[11] or $Eu(Pd_{1-x}Pt_x)_2Si_2$.[12] In the case of $CeCu_2Ge_2$ and $CeCu_2Si_2$, where T_K and T_0 seem to be of the same order of magnitude, we show that the pressure dependence of the $A(P)$ coefficient and the residual resistance are driven by the change in the degeneracy of the f states.

The paper is organized as follows. Section II explains briefly the slave boson (SB) formalism for the Anderson model and defines its low- and high-temperature scales T_0 and T_K. This section provides also the relationship between the c DOS and the relative magnitude of T_0 and T_K, discusses the effects of the magnetic field, and shows how to express the transport coefficients in terms of T/T_0. In Sec. III we discuss the relevance of these results for the experimental data on various intermetallic compounds in which the ratio T_0/T_K can be much smaller or larger than one. For the case $T_0 \simeq T_K$, we discuss the pressure anomalies in the A coefficient and the residual resistance induced by the changes in the effective degeneracy of the f states.

II. SLAVE BOSON SOLUTION OF THE PERIODIC ANDERSON MODEL

A. Mean-field self-consistent equations in the limit $U\rightarrow\infty$

The periodic Anderson model (PAM) Hamiltonian is written in the limit of an infinite correlation between f electrons $U=+\infty$, as

$$H = \sum_{\mathbf{k}\sigma} \epsilon_{\mathbf{k}} c^{\dagger}_{\mathbf{k}\sigma} c_{\mathbf{k}\sigma} + E_f \sum_{i\sigma} f^{\dagger}_{i\sigma} f_{i\sigma} + V \sum_{i\sigma} [c^{\dagger}_{i\sigma} f_{i\sigma} + f^{\dagger}_{i\sigma} c_{i\sigma}] - \mu \sum_{i\sigma} [f^{\dagger}_{i\sigma} f_{i\sigma} + c^{\dagger}_{i\sigma} c_{i\sigma}] + h \sum_{i} [g_c (c^{\dagger}_{i\uparrow} c_{i\uparrow} - c^{\dagger}_{i\downarrow} c_{i\downarrow}) + g_f (f^{\dagger}_{i\uparrow} f_{i\uparrow} - f^{\dagger}_{i\downarrow} f_{i\downarrow})], \quad (1)$$

where $c_{i\sigma}$ and $f_{i\sigma}$ are annihilation operators for c and f electrons, i is the site index, $\sigma=\uparrow,\downarrow$ is the spin component, h is an external magnetic field, and g_c and g_f are the Landé factors for c and f orbitals, respectively. The c orbital describes the conduction band with energy levels $\epsilon_{\mathbf{k}}$, where $\mathbf{k}$ is the momentum component in the reciprocal space, the localized f orbitals are characterized by energy level E_f, and the local hybridization between the two orbitals is specified by the matrix element V. The infinite Coulomb repulsion restricts the occupation of the f states to $n_f \leq 1$ and we use the chemical potential μ to fix the total electronic occupation per site to $n=n_c+n_f$. The unperturbed c DOS is $\rho_0(\omega)=1/\mathcal{N}\Sigma_{\mathbf{k}}\delta(\omega-\epsilon_{\mathbf{k}})$, where $\mathcal{N}$ is the number of lattice sites. In the following, ρ_0 will be characterized by a half bandwidth D. Typical band shapes and fillings considered in this work are shown in Fig. 1. All the energies (except the excitation energies) are measured with respect to the center of the c band (see Fig. 1). The effective degeneracy of the model is determined by the lowest spin-orbit state or the additional crystal-field splitting of the f states of the Ce and Yb ions. This degeneracy can be changed by temperature, pressure or chemical pressure. Here, we consider an effective spin-1/2 model.

The model defined by Eq. (1) is solved for an arbitrary c DOS by the slave boson mean-field (MF) approximation,[13,14] which represents the f states by the product of spinless bosons $b^{\dagger}_i$ and auxiliary fermions of spin $\sigma=\uparrow,\downarrow$, $d^{\dagger}_{i\sigma}$. By

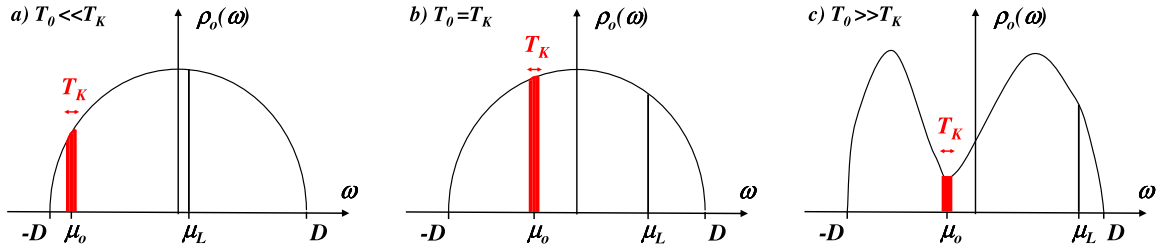

FIG. 1. (Color online) Schematic plot of the noninteracting c DOS $\rho_0(\omega)$. (a) For a regular c DOS and far from the electronic half-filling, we find $T_0 \ll T_K$. Close to the half-filling, T_0/T_K depends on the shape of the c DOS around the renormalized chemical potential μ: (b) $\rho_0(\omega)$ is nearly constant for $\omega \sim \mu$ and $T_0 \sim T_K$. (c) μ is close to a minimum of $\rho_0(\omega)$ and $T_0 \gg T_K$. Here, $\mu_0 \approx \mu$ is the chemical potential of $n_c = n-1$ noninteracting c electrons ("small Fermi surface") and μ_L is the chemical potential of $n_c = n$ noninteracting c electrons ("large Fermi surface").

definition, these auxiliary particle operators create the local f states with no electron and one σ-spin electron, respectively; $|0\rangle_i^f \to b_i^\dagger |0\rangle_i$ and $|\sigma\rangle_i^f \to d_{i\sigma}^\dagger |0\rangle_i$. The electronic operators are related to the auxiliary operators as $f_{i\sigma} = b_i^\dagger d_{i\sigma}$, which leads to the local identities $f_{i\sigma}^\dagger f_{i\sigma} = d_{i\sigma}^\dagger d_{i\sigma}$. The doubly occupied state $|\uparrow\downarrow\rangle_i^f$ is forbidden in the limit $U \to \infty$. The anticommutation relations for f operators as well as the physical Hilbert space are recovered by enforcing the local constraints $b_i^\dagger b_i + \Sigma_\sigma d_{i\sigma}^\dagger d_{i\sigma} = 1$. The latter is satisfied by introducing the time-dependent Lagrange multipliers $\lambda_i(\tau)$. Assuming $g_c \ll g_f$, we set $g_c = 0$ and $g_f = 1$, replace $h g_f \to h$, and rewrite the PAM Hamiltonian (1) in terms of auxiliary fermionic and bosonic operators,

$$H_{\mathrm{SB}} = \sum_{\mathbf{k}\sigma} \epsilon_{\mathbf{k}} c_{\mathbf{k}\sigma}^\dagger c_{\mathbf{k}\sigma} + V \sum_{i\sigma} [b_i^\dagger c_{i\sigma}^\dagger d_{i\sigma} + b_i d_{i\sigma}^\dagger c_{i\sigma}] - \mu \sum_{i\sigma} c_{i\sigma}^\dagger c_{i\sigma} + h \sum_i (d_{i\uparrow}^\dagger d_{i\uparrow} - d_{i\downarrow}^\dagger d_{i\downarrow}) + (E_f - \mu) \sum_i (1 - b_i^\dagger b_i) + \sum_i \lambda_i [b_i^\dagger b_i - 1 + \sum_\sigma d_{i\sigma}^\dagger d_{i\sigma}]. \quad (2)$$

Since the slave boson Hamiltonian (2) is invariant under the local gauge transformation $b_i \to b_i e^{i\theta_i}$, $d_{i\sigma} \to d_{i\sigma} e^{i\theta_i}$, we choose the gauge such that the bosonic fields are real $b_i = b_i^\dagger \equiv r_i$. Finally, we make the MF approximation, assuming that the boson fields and the Lagrange multipliers are homogeneous and spin-independent constants $r_i \equiv r$ and $\lambda_i \equiv \lambda$. Within this MF approach, which is exact in the limit of a large number of spin components, the Hamiltonian (2) becomes quadratic,

$$H_{\mathrm{SB}}^{\mathrm{MF}} = \sum_{\mathbf{k}\sigma} \left[\epsilon_{\mathbf{k}} c_{\mathbf{k}\sigma}^\dagger c_{\mathbf{k}\sigma} + rV(c_{\mathbf{k}\sigma}^\dagger d_{\mathbf{k}\sigma} + d_{\mathbf{k}\sigma}^\dagger c_{\mathbf{k}\sigma}) - \mu c_{\mathbf{k}\sigma}^\dagger c_{\mathbf{k}\sigma} + \lambda_\sigma d_{\mathbf{k}\sigma}^\dagger d_{\mathbf{k}\sigma} + \frac{E_f - \lambda - \mu}{2}(1 - r^2) \right], \quad (3)$$

where

$$\lambda_\uparrow \equiv \lambda + h, \quad (4)$$

$$\lambda_\downarrow \equiv \lambda - h. \quad (5)$$

In the presence of the magnetic field h, the Lagrange multipliers are shifted by $\pm h$ but the up- and down-spin states remain decoupled. The self-consistent solution is obtained by minimizing the free energy $\beta \mathcal{F}(r,\lambda) \equiv -\ln \mathrm{Tr} e^{-\beta H}$ with respect to r and λ. From $\partial \mathcal{F}(r,\lambda)/\partial r = 0$ and $\partial \mathcal{F}(r,\lambda)/\partial \lambda = 0$, we obtain

$$2r(E_f - \lambda - \mu) = \frac{V}{\mathcal{N}} \sum_{\mathbf{k}\sigma} \langle c_{\mathbf{k}\sigma}^\dagger d_{\mathbf{k}\sigma} + d_{\mathbf{k}\sigma}^\dagger c_{\mathbf{k}\sigma} \rangle, \quad (6)$$

$$r^2 = 1 - \frac{1}{\mathcal{N}} \sum_{\mathbf{k}\sigma} \langle d_{\mathbf{k}\sigma}^\dagger d_{\mathbf{k}\sigma} \rangle, \quad (7)$$

where $\langle \cdots \rangle$ is the thermal average with respect to the MF Hamiltonian (3). The total electron occupation per site is

$$n = \frac{1}{\mathcal{N}} \sum_{i\sigma} \langle d_{i\sigma}^\dagger d_{i\sigma} + c_{i\sigma}^\dagger c_{i\sigma} \rangle \equiv n_f + n_c. \quad (8)$$

Here, $n_f \equiv 1/\mathcal{N} \Sigma_{i\sigma} \langle f_{i\sigma}^\dagger f_{i\sigma} \rangle = 1/\mathcal{N} \Sigma_{i\sigma} \langle d_{i\sigma}^\dagger d_{i\sigma} \rangle$ and $n_c \equiv 1/\mathcal{N} \Sigma_{i\sigma} \langle c_{i\sigma}^\dagger c_{i\sigma} \rangle$, are the average occupations per site for f and c orbitals, respectively. Using the relationship between the slave boson amplitude and the total electronic occupation,

$$n_f = 1 - r^2, \quad (9)$$

$$n_c = n - n_f, \quad (10)$$

the self-consistency (6)–(8) can be written for $r \neq 0$ as

$$\frac{\lambda + \mu - E_f}{V^2} = \frac{1}{rV} \sum_\sigma \int_{-\infty}^{+\infty} \rho_{dc}^\sigma(\omega) n_F(\omega) d\omega, \quad (11)$$

$$n_f = \sum_\sigma \int_{-\infty}^{+\infty} \rho_d^\sigma(\omega) n_F(\omega) d\omega, \quad (12)$$

$$n_c = \sum_\sigma \int_{-\infty}^{+\infty} \rho_c^\sigma(\omega) n_F(\omega) d\omega, \quad (13)$$

where $n_F(\omega) \equiv 1/[1 + e^{\beta\omega}]$ is the Fermi function and ρ_{dc}^σ, ρ_d^σ, and ρ_c^σ are the spectral densities of the local single-particle Green's functions of a given spin component. The Green's functions are defined in the usual way as thermal averages of the (imaginary) time-ordered products of the appropriate creation and annihilation operators. For the quadratic MF Hamiltonian (3), the Green's functions for $r \neq 0$ are easily

calculated by the equations of motion, which yields[15]

$$\rho_{dc}^{\sigma}(\omega) \equiv -\frac{1}{\pi}\mathrm{Im}\, G_{dc}^{\sigma}(\omega) = \frac{rV}{\omega-\lambda_{\sigma}}\rho_c^{\sigma}(\omega), \tag{14}$$

$$\rho_{d}^{\sigma}(\omega) \equiv -\frac{1}{\pi}\mathrm{Im}\, G_{d}^{\sigma}(\omega) = \frac{r^2V^2}{(\omega-\lambda_{\sigma})^2}\rho_c^{\sigma}(\omega), \tag{15}$$

$$\rho_{c}^{\sigma}(\omega) \equiv -\frac{1}{\pi}\mathrm{Im}\, G_{c}^{\sigma}(\omega) = \rho_0\left(\omega+\mu-\frac{r^2V^2}{\omega-\lambda_{\sigma}}\right). \tag{16}$$

In what follows, we analyze the MF slave boson solution and discuss the effects of the band structure.

B. High-temperature solution

At high enough temperatures, the self-consistency (6)–(10) have only a trivial $r=\lambda=0$ solution, i.e., the effective MF hybridization in Eq. (3) vanishes $rV=0$. This solution describes a system of decoupled f and c electrons. For $h=0$ and $E_f<\mu$, each lattice site is occupied by a single f electron of spin σ and there are $n_c=n-1$ conduction electrons (per site) with the c DOS given by $\rho_0(\epsilon)$. The Fermi surface (FS) encloses $n_c=n-1$ points in the k space, i.e., the $r=0$ state occupies a "small" Fermi volume that includes the "light" c electrons but not the localized f states. The magnetic susceptibility is Curie-type provided the direct effect of h on the conduction electrons is neglected. (The Pauli-type susceptibility of c electrons is negligible with respect to the Curie contribution of the f states.) As long as the c states are highly degenerate $T \ll D$, their entropy is much smaller than the entropy of the localized f states, and the overall entropy per site is approximately given by $S=\ln 2$. In the presence of a large magnetic field, the degeneracy of the f states is lifted and the system acquires additional Zeeman energy.

Even though the trivial $r=\lambda=0$ solution does not provide a quantitative description of the PAM at high temperatures, it captures the essential qualitative point: it represents the whole system in terms of two well-defined but separated subsystems. A more realistic approach would take into account the small coupling between the c and f electrons and treat it as a perturbation. This would reduce the average f occupation to $n_f<1$, give the Curie Weiss rather than the Curie susceptibility, and obtain the transport properties from the scattering of "light" c electrons on the f ions. The resistivity calculated in such a way has logarithmic corrections to the high-temperature spin-disorder limit. However, both the trivial slave boson solution and the perturbative one break down at sufficiently low temperatures.

Remarkably, the Kondo scale T_K defined by the high-temperature perturbation expansion agrees with the characteristic temperature at which the nontrivial solution of the slave boson equations emerges. In what follows, we analyze the nontrivial self-consistent solution of Eqs. (6)–(10) for the spin-1/2 model and show that it captures the main features of the experimental data on Ce, Eu, and Yb intermetallic compounds at low temperatures. The generalization to an arbitrary SU(N) symmetric Anderson model or the model with the CF split f states is straightforward (see Appendix A).

C. Kondo temperature T_K

The nontrivial $r\neq 0$ solution of the slave boson equations is found below some critical temperature which defines the Kondo scale T_K of the periodic Anderson model. For a given set of parameters and total occupation n, the Kondo scale is obtained from the $r\,\lambda \to 0$ limit of Eqs. (6)–(8). This gives, for $h=0$,

$$\frac{2}{J(\mu)} = \int_{-\infty}^{+\infty}\frac{\rho_0(\omega+\mu)\tanh(\omega/2T_K)}{\omega}d\omega, \tag{17}$$

$$n_f = 2\int_{-\infty}^{+\infty} d\omega\delta(\omega-\lambda)n_F(\omega) = 1, \tag{18}$$

$$n_c = n-1 = 2\int_{-\infty}^{+\infty} d\omega\rho_0(\omega+\mu)n_F(\omega), \tag{19}$$

where we introduced the Kondo coupling constant,

$$J(\mu) \equiv \frac{2V^2}{\mu-E_f}. \tag{20}$$

Assuming that T_K vanishes continuously and taking the limit $T_K \to 0$ yields the critical coupling

$$\frac{2}{J_c} = \int_{-\infty}^{+\infty} d\omega\frac{\rho_0(\omega+\mu)}{|\omega|}. \tag{21}$$

For a regular DOS $\rho_0(\mu)\neq 0$, the right-hand side of Eq. (21) diverges logarithmically such that $J_c=0$ and any finite coupling leads to $T_K>0$. At T_K, the high-temperature $r=0$ phase with large paramagnetic entropy is destabilized by a transition to the low-entropy Fermi-liquid phase. The Kondo scale given by Eq. (17) coincides with the solution of the scaling equations for the SU(2) single-impurity Kondo model.[6]

The physical interpretation of the emergence of the nontrivial slave boson solution is made by the analogy with the single-impurity case. We assume that the high-temperature solution of the lattice describes a system of localized f and itinerant c electrons with small FS and that the correction to the $r=0$ solution can be found by the perturbation theory in terms of $J(\mu)$. For $T>T_K$, the hybridization energy is small with respect to the entropic contribution to the free energy due to the degenerate f states. Thus, the total free energy of the system $\mathcal{F}=E-TS$ is minimized at high temperatures by the paramagnetic configuration in which the f states are very weakly coupled to the c states. For $T \leq T_K$, the entropic contribution is reduced below the hybridization energy and the paramagnetic configuration becomes thermodynamically unstable. At T_K, the crossover between the local moment and a local singlet state takes place.

In the case of an unperturbed c DOS with a pseudogap at μ, $\rho_0(\mu)=0$, Eqs. (11)–(13) yield the solution with finite J_c which separates two different low-temperature regimes. For $J>J_c$, the $r\neq 0$ solution emerges at temperature T_K which is the same as in the $\rho_0(\mu)\neq 0$ case. But for $J<J_c$, the $r=0$ solution persists down to $T=0$ such that the paramagnetic entropy is not removed by Kondo scattering. If the coupling is tuned by pressure or doping, a quantum phase transition

can be induced at the critical value J_c (or V_c). In the case of c DOS with a gap $\Delta_g \ll D$ around the Fermi level, we find $J_c \propto D/ln[D/\Delta_g]$. A pseudogap centered at the chemical potential μ and characterized by a single energy scale D gives $J_c \propto D$. The power-law singularity $\rho_0(\omega)=R_0|\omega|^\eta$ gives $J_c=2\eta D/(\eta+1)$, which is the Whithoff and Fradkin[6] result.[7] [The constant R_0 follows from the normalization condition $\int_{-D}^{D}\rho_0(\omega)=1$.]

To find T_K at finite $\rho_0(\mu)$, we use the Sommerfeld expansion of Eq. (17) which gives in the $T_K \ll D$ limit the result

$$T_K = \alpha_0 (D^2 - \mu_0^2)^{1/2} F_K e^{-1/J(\mu_0)\rho_0(\mu_0)}, \tag{22}$$

where

$$F_K = \exp\left[\int_{-(D+\mu_0)}^{D-\mu_0} \frac{\rho_0(\mu_0+\omega)-\rho_0(\mu_0)}{2|\omega|\rho_0(\mu_0)} d\omega\right]. \tag{23}$$

ω is measured with respect to μ, $\alpha_0=1.13$ is a numerical constant, and μ_0 is defined by the integral

$$\frac{n_c}{2} = \frac{n-1}{2} = \int_{-D}^{\mu_0} \rho_0(\omega) d\omega. \tag{24}$$

By definition, μ_0 is the Fermi level of n_c noninteracting electrons which have a "small" FS. The result given by Eq. (22) is derived in Ref. 16 for a Kondo lattice with an analytic DOS. It also holds for $\rho_0(\omega)$ with an algebraic singularity close to μ_0.

The Kondo temperature T_K defined in Eq. (17) characterizes a second-order phase transition. We are aware that this transition is an artifact of the slave boson MF approximation and that an exact theory would lead to a crossover instead. Experimentally, the Kondo temperature T_K is sometimes estimated from the resistivity measurements, which show a maximum around T_K, or from the specific-heat measurements, where T_K is identified as the temperature at which the magnetic entropy (per impurity) becomes a substantial fraction of ln 2, say $S \simeq 0.5$ ln 2 (see Fig. 2). Note that with this definition of T_K from the magnetic entropy, we implicitly neglect the collective freezing of the entropy which is related to the Ruderman-Kittel-Kasuya-Yosida interaction.

The fact that the Anderson lattice and the single-impurity Anderson model have the same Kondo scale indicates that in both cases, T_K separates the paramagnetic high-entropy phase from the low-entropy phase in which the conduction electrons start forming an incoherent screening clouds which reduce the local f moment in each unit cell (see Fig. 1). At temperatures at which the c and f states form a coherent band and local screening clouds become correlated, the hybridization V cannot be considered as a perturbation. For $T \ll T_K$, the Hamiltonian has to be diagonalized by nonperturbative methods and the slave boson solution provides a reasonable description of the renormalized ground state. Close to the ground state, the low-energy excitations of a periodic system are Bloch waves and we expect them to be characterized by a FL scale T_0. The question is that how is T_0 related to T_K.

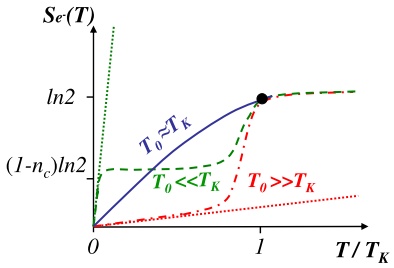

FIG. 2. (Color online) Schematic plot of the electronic contribution to the entropy S_{e^-} as a function of the normalized temperature T/T_K for three cases: $T_0 \gg T_K$ (red dash-dotted line), $T_0 \approx T_K$ (blue solid line), and $T_0 \ll T_K$ (green-dashed line). The dotted lines indicate the linear Fermi-liquid regime $S_{e^-}(T)=T/T_0$, with a rescaled slope T_K/T_0. For $T>T_K$, the three curves are identical, reflecting the linear contribution from the conduction band $S_{e^-}(T)=\ln 2+T/D$. The black dot refers to a standard determination of T_K from the electronic entropy: $S_{e^-}(T_K)=x$ ln 2. On this schematic plot, we used $x=1$, which gives T_K as defined by the slave boson ($r=0$) solution. Experimentally, where T_K is defined by the crossover, one usually takes $x=1/2$.

D. Fermi-liquid scale T_0

The emergence of a strongly coupled $f-c$ fluid at T_K does not imply that Kondo scale characterizes the behavior of such a fluid close to the ground state. Electrons described by Eq. (3) form at $T=0$ a coherent Fermi liquid with an energy scale T_0, which is defined in the absence of a magnetic field as

$$T_0 \equiv \frac{1}{\rho^{\uparrow}(\mu)} = \frac{1}{\rho^{\downarrow}(\mu)}, \tag{25}$$

where $\rho^\sigma(\mu) \equiv \rho_c^\sigma(\mu)+\rho_f^\sigma(\mu)$ is the renormalized density of electronic states at the Fermi level. The scale T_0 is relevant for the $T \to 0$ properties of the periodic Anderson model; it determines the static spin susceptibility $\chi_{\rm loc}(T=0) \sim 1/T_0$, the specific-heat coefficient $\gamma = C_V/T \sim 1/T_0$, and appears in the transport coefficients[17] which are given by simple powers of reduced temperature T/T_0. The slave boson result for T_0 is computed from Eqs. (11)–(16) at $T=0$, which gives

$$\frac{E_f-\lambda-\mu}{2V^2} = \int_{-\infty}^{0} \frac{1}{\omega-\lambda} \rho_0\left(\omega+\mu-\frac{r^2V^2}{\omega-\lambda}\right) d\omega, \tag{26}$$

$$\frac{n_c+n_f}{2} = \int_{-\infty}^{0} \left[1+\frac{r^2V^2}{(\omega-\lambda)^2}\right] \rho_0\left(\omega+\mu-\frac{r^2V^2}{\omega-\lambda}\right) d\omega = \int_{-\infty}^{\mu_L} \rho_0(\omega) d\omega, \tag{27}$$

where $\rho_0(\omega)$ is the unperturbed c DOS and μ_L is the chemical potential of $n=n_c+n_f$ noninteracting electrons. We have

$$\mu_L \equiv \mu + \frac{r^2V^2}{\lambda}, \tag{28}$$

which defines the shift in the chemical potential due to the enlargement of the Fermi volume of hybridized ($r \neq 0$) system with n particles with respect to the Fermi volume of the

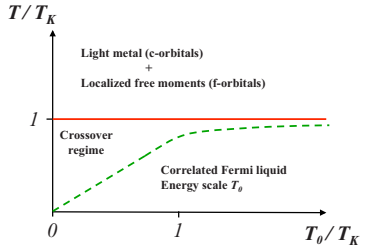

FIG. 3. (Color online) Schematic phase diagram of the PAM. The reduced temperature T/T_K is plotted versus T_0/T_K, which is considered as a tunable parameter that can vary with the electronic filling, magnetic field, and/or the shape of the noninteracting DOS. The crossover regime can be nonuniversal or non-Fermi liquid.

noninteracting ($r=0$) band with $n-1$ particles, $\Delta\mu \equiv \mu_L - \mu = r^2V^2/\lambda$. (This interpretation of $\Delta\mu$ neglects the width of the free-electron distribution function at temperature T_K with respect to D and assumes $\mu \simeq \mu_0$, which holds for $n_f \simeq 1$.) The low-temperature FS is "enlarged" with respect to the high-temperature one, as it has to accommodate n_f additional f electrons. Equations (15), (16), and (28) yield

$$\rho(\mu) = \left[1 + \left(\frac{\Delta\mu}{rV}\right)^2\right]\rho_0(\mu_L), \tag{29}$$

which shows that $\rho(\mu)$ and T_0 depend on the shape of the unperturbed c DOS and on the total number of particles. In the FL regime, the entropy behaves as T/T_0, the susceptibility is constant, and transport coefficients are given by simple power laws of T/T_0. The schematic phase diagram of a system with $T_K \neq T_0$ is shown schematically in Fig. 3.

The effect of the c DOS can be computed analytically in the $V \ll D$ limit, assuming that μ is close to μ_0. Since μ_L corresponds to n noninteracting electrons ("large" FS) and μ_0 to $n_c \sim n-1$ electrons ("small" FS), we approximate $\Delta\mu \propto D$ (see Fig. 1). In the limit $rV/D \ll 1$, the MFs (26) and (27) give

$$\frac{E_f - \lambda - \mu}{2V^2} = \rho_0(\mu)\ln\left(\frac{r^2V^2}{(D+\mu)\Delta\mu}\right) - \int_{-(D+\mu)}^{\Delta\mu} \frac{\rho_0(\mu+\omega) - \rho_0(\mu)}{|\omega|} d\omega, \tag{30}$$

$$\frac{n_c + n_f}{2} = \int_{-(D+\mu)}^{\Delta\mu} \rho_0(\mu+\omega)d\omega, \tag{31}$$

where we neglected the corrections of order $(rV/D)^2$. Solving Eqs. (30) and (31) for λ yields

$$\lambda \simeq \frac{r^2V^2}{\Delta\mu} \simeq (D+\mu_0)F_0 e^{-1/J(\mu_0)\rho_0(\mu_0)}, \tag{32}$$

where

$$F_0 = \exp\left[\int_{-(D+\mu_0)}^{\Delta\mu} \frac{\rho_0(\mu_0+\omega) - \rho_0(\mu_0)}{|\omega|\rho_0(\mu_0)} d\omega\right]. \tag{33}$$

The scale T_0 of a system of particles described by the periodic Anderson model close to the ground state is obtained from Eqs. (25), (29), and (32) as

$$T_0 = \frac{r^2V^2}{(\Delta\mu)^2}\frac{1}{\rho_0(\mu_L)} = \frac{D+\mu_0}{\Delta\mu}\frac{F_0}{\rho_0(\mu_L)} e^{-1/J(\mu_0)\rho_0(\mu_0)}. \tag{34}$$

The scales T_0 and T_K have the same exponential dependence on the coupling constant $J(\mu_0)$ but their prefactors are not affected by $\rho_0(\omega)$ in the same way and can differ considerably. The ratio T_0/T_K which is constant for a given set of parameters can be changed by applying pressure or magnetic field.

At temperatures low with respect to $T_{\mathrm{FL}} = \min\{T_0, T_K\}$, the system behaves as a Fermi liquid (provided we are not too close to the Kondo insulating state) but the crossover from the high-temperature to the low-temperature regime proceeds differently for $T_0 \ll T_K$ than for $T_0 \gg T_K$. This is shown schematically in Figs. 2 and 3. If $T_0 \ll T_K$, we have $T_{\mathrm{FL}} = T_0$ and, for $T_0 < T < T_K$, the system exhibits an extended nonuniversal behavior. If the electronic occupation n_c is neither too small nor too close to half-filling, the MF solution of the slave boson equations[16] predicts the entropy with a plateau at about $(1-n_c)\ln 2$ (see Fig. 2), which characterizes $1-n_c$ unscreened magnetic ions. If $T_0 \gg T_K$, the high-temperature perturbative regime persists all the way down to T_K, where the properties change abruptly and the system enters the FL phase characterized by T_0. Only for $T_0 \sim T_K$, the lattice system is characterized by a single energy scale, as in the single-impurity case.

E. Comparison of the Fermi liquid and the Kondo scales

The Kondo coupling $J(\mu)$ defined by Eq. (20) is always smaller than the half bandwidth D of the noninteracting c DOS such that T_K and T_0 are exponentially small due to the factor $\exp\{-1/J(\mu_0)\rho_0(\mu_0)\}$. The analytic expressions given by Eqs. (22) and (34) yield the result

$$\frac{T_0}{T_K} = \left(\frac{D+\mu_0}{D-\mu_0}\right)^{1/2} \frac{1}{\alpha_0\rho_0(\mu_L)\Delta\mu}\frac{F_0}{F_K}, \tag{35}$$

which does not depend on the Kondo coupling $J(\mu)$ but, as discussed previously,[16] varies with the electronic occupation and with the shape of the noninteracting c DOS. Electronic filling effects have been discussed using the MF analysis of the Kondo lattice[16] and the dynamical mean-field theory solution of the periodic Anderson model.[18] In the limit $n_c \to 0$ ($n \approx 1$), the first factor $D+\mu_0$ vanishes and $T_0 \ll T_K$ [see Fig. 1(a)]. Another physically relevant case is found in the limit $n_c \approx 1$, which corresponds to a Kondo insulator with the vanishingly small $\rho_0(\mu_L)$. Equation (35) yields $T_0 \gg T_K$ and the breakdown of the FL laws is neither due to the proliferation of the quasiparticle (QP) excitations (controlled by T_0) nor to the thermal destruction of the Kondo screening (controlled by T_K) but is due to the proximity of the chemical potential to the hybridization gap in the DOS.

We consider now in more detail the effects due to the shape variation of $\rho_0(\omega)$. In order to separate this effect from the electronic occupation effects,[19,20] we assume that n_c is close to 1 (but not at half-filling exactly, so that the system is metallic). The first two factors on the right-hand side of Eq. (35) are then of the order 1 such that $T_0/T_K \approx F_0/F_K$. Assuming $\Delta\mu \approx D-\mu_0$, we obtain from Eqs. (23) and (33) a simple relation

$$\frac{T_0}{T_K} \sim \exp\left[\int_{-(D+\mu_0)}^{D-\mu_0} \frac{\rho_0(\mu_0+\omega)-\rho_0(\mu_0)}{2|\omega|\rho_0(\mu_0)} d\omega\right], \quad (36)$$

which describes the dependence of T_0/T_K on the specific form of ρ_0. A constant ρ_0 gives $T_0 \sim T_K$, which explains the T/T_K scaling observed in some heavy fermion compounds. If μ_0 is close to a local maximum of $\rho_0(\omega)$, the integrand in Eq. (36) is negative in the main part of the integration range, such that $T_0 \leq T_K$, as found in the systems with the "protracted screening."[9,18] A sharp spike in $\rho_0(\omega)$ close to μ_0 would exponentially reduce T_0 with respect to T_K. On the other hand, if μ_0 is close to a local minimum [see Fig. 1(b)] one finds $T_0 \gg T_K$, which could be understood by the following intuitive argument. The incoherent Kondo cloud which begins to form at $T \approx T_K$ involves a few conduction states around the Fermi energy μ_0. These states are part of the conduction band with a "small" FS (the FS of $n_c=n-1$ noninteracting electrons). When temperature decreases much below T_K, the local f orbitals hybridize with the conduction electrons to form a coherent Fermi liquid which is characterized by a "large" Fermi surface (the FS of n noninteracting electrons). Thus, T_0 is affected by all the states between the "small" and the "large" FS, as well as some additional holes inside the "small" FS.[16] For $n_c \simeq 1$ and μ_0 close to the minimum of $\rho_0(\omega)$, the low-temperature increase in the Fermi volume leads to the DOS which is much larger than the one used to evaluate T_K [see Fig. 1(c)]. In that case, the formation of the Fermi liquid is "self-amplified," yielding $T_0 \gg T_K$. We recall that for $T_0 \neq T_K$, the FL regime sets in at temperatures that are the smaller than either T_0 or T_K.

We are aware that corrections to MF slave boson analysis might occur from a more accurate treatment of the model; nevertheless, since the SB approximation is known to be correct at low energy, we expect such corrections to provide a similar integral expression, where the $1/|\omega|$ divergency would be smoothed out at height frequencies. The analytical expression (36) still provides a good quantitative estimation of the band shape effect in the vicinity of the chemical potential. The relative magnitude of T_0 and T_K is related to the functional form of $\rho_0(\omega)$ around $\omega=\mu$.

F. Effect of a magnetic field

We next consider the slave boson solution in the presence of an external magnetic field which couples to the f orbitals. The direct effect on the c electrons is neglected, even though they can be polarized due to the interaction with f electrons. In the linear-response regime, the local magnetization of the f orbitals $m_z(h) \equiv \frac{1}{2N}\Sigma_i(\langle f_{i\uparrow}^\dagger f_{i\uparrow}\rangle - \langle f_{i\downarrow}^\dagger f_{i\downarrow}\rangle)$ is proportional to the applied field h and, in the Kubo formalism,[21] the proportionality factor is equal to the local static susceptibility computed in the absence of the field. At $T=0$, the magnetization is $m_z(h) \propto h/T_0$, where T_0 is defined by Eq. (25). Going beyond the linear response, the critical magnetic field $h_c(T)$ is defined at a given temperature by the transition between the $r \neq 0$ and $r=0$ states. Solving the MFs (11)–(13) in the $r \to 0$ limit and using the definition of the Kondo coupling $J(\mu)$ in Eq. (20), we find for $n_f=1$

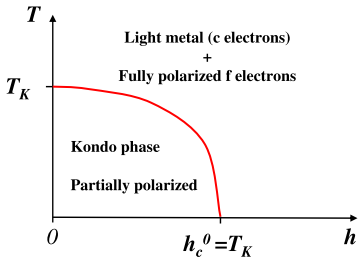

FIG. 4. (Color online) Schematic phase diagram of the PAM as a function of a magnetic field h. The red solid line indicates $h_c(T)$ which separates the trivial $r=0$ solution from the nontrivial one $r \neq 0$.

$$\frac{1}{J(\mu)} = \int_{-\infty}^{+\infty} \frac{\omega}{\omega^2 - h_c^2} \rho_0(\omega+\mu) \tanh\left[\frac{\omega}{2T}\right] d\omega, \quad (37)$$

which yields $h_c \neq 0$ for any regular $\rho_0(\omega)$. Unlike the zero-field result (21), which is logarithmically singular and gives $J_c=0$ for any finite $\rho_0(\mu)$, Eq. (37) yields $J_c \neq 0$ for any finite field. For $h \geq h_c(T)$, there is only the trivial $r=0$ solution which describes ferromagnetically polarized f moments decoupled from the conduction band (see Fig. 4). For $h \leq h_c(T)$, the equations have a nontrivial $r \neq 0$ solution which describes a partially polarized Fermi liquid. At $T=0$, the weak-coupling limit ($J \ll D$) yields the universal relation

$$h_c^0 \equiv h_c(T=0) = \alpha_0^{-1} F_K e^{-1/J(\mu)\rho_0(\mu)} = \alpha_0^{-1} T_K. \quad (38)$$

Since $\alpha_0=1.13$, we have $h_c^0 \simeq T_K$. At finite temperatures, the solution of Eq. (37) with constant c DOS yields the critical line

$$[h_c(T)/h_c^0]^2 + [T/T_K]^2 = 1, \quad (39)$$

which separates the trivial solution (the decoupled phase) from the nontrivial one (the FL phase) and holds for any $J(\mu)$ and filling n. The critical line $h_c(T)$ obtained for a constant c DOS is represented schematically in Fig. 4. The same relation is also found at half-filling, for any c DOS. In general, we expect a "nearly" universal phase boundary, with some small deviations due to the structure of the c DOS *and* the particle-hole asymmetry. Studying the development of the system as a function of temperature at constant field gives the critical temperature $T_K(h)$. Changing the field at constant temperature gives $h_c(T)$.

The magnetization $m_z(h)$ obtained from the slave boson solution at $T=0$ is plotted in Fig. 5 as a function of reduced magnetic field h/T_K for three typical cases: $T_0 \ll T_K$, $T_0 \approx T_K$, and $T_0 \gg T_K$. A nonconstant c DOS leads to different types of magnetization curves which resemble the temperature dependence of the entropy depicted in Fig. 2 (with the T/T_K axis replaced by h/h_c^0). For $h < \min\{T_0, T_K\}$, the system

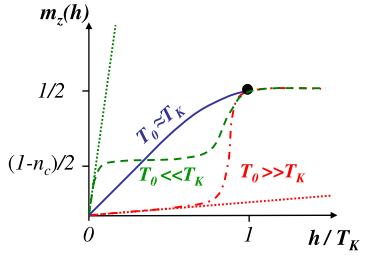

FIG. 5. (Color online) Schematic plot of the magnetization m_z as a function of reduced magnetic field h/T_K for $T_0 \gg T_K$ (red dash-dotted line), $T_0 \approx T_K$ (blue solid line), and $T_0 \ll T_K$ (green-dashed line). The dotted lines indicate the initial slope in the linear-response regime, where $m_z(h)=h/T_0$. The black dot refers to the complete polarization of the local f electrons, with $m_z=1/2$, which occurs at the critical field $h_c^0=T_K$.

is in the linear-response regime shown in Fig. 5 by dotted lines; the slope of $m_z(h)$ is T_K/T_0, when plotted versus h/T_K. This regime is analogous to the FL regime described from the entropy. In higher fields, the behavior of the slave boson solution depends on the ratio T_0/T_K. For $T_0 \ll T_K$, the $T=0$ magnetization is linear for small fields and then saturates. For $T_0 < h < T_K$, the magnetization might have a plateau which signifies a saturated FL ($r \neq 0$) with a "large" FS. At very high fields $h \geq T_K \sim h_c^0$, the magnetization becomes a universal function of h/h_c^0. In the opposite case $T_K \ll T_0$, the low-field limit gives $m_z(h) \propto h/T_0$ and the initial slope appears very small when plotted versus h/h_c^0. Once the field exceeds the critical value $h_c^0 \sim T_K$, the local moments are unscreened and $m_z(h)$ rises rapidly toward the free-ion value. Thus, at about $h \simeq h_c^0$ such systems exhibit a metamagnetic transition from an unpolarized Fermi liquid to the polarized spin lattice (the $r=0$ phase). Of course, this simple consideration should be corrected for direct and indirect effects due to the conducting sea.

G. Stability of the Fermi liquid toward magnetic fluctuations

The SB solution of the periodic Anderson model with infinite U accounts very well for the Kondo effect in intermetallic compounds with Ce and Yb ions. As shown in Secs. II B–II F, this solution explains the crossover into the FL regime and the reduction in large paramagnetic entropy at the crossover temperature. However, the effective model defined by Eq. (3) cannot describe the removal of entropy by a magnetic transition nor the competition between the Kondo effect and magnetism.[22–24] In our treatment, the localized boson is associated with the $4f^0$ configuration and, on the mean field level, its condensation marks the formation of hybridized states with large FS. Above the condensation temperature $T \geq T_K$, the f and c states are completely decoupled and the FS is small. From the preceding discussion, it is clear that the characteristic temperatures T_0 and T_K calculated for the SB Hamiltonian (3) are not taking into account the intersite magnetic fluctuations. The enhancement of the FL scale that seems to occur when the system is driven toward the magnetic boundary from the FL side cannot be described by the simple SB solution of the infinite-U PAM used in this paper.

One way of extending the SB treatment to magnetic instabilities would be to start from a finite-U PAM and, then, exclude from the Hilbert space all the states with more than one f electron per lattice site. The effective model generated in such a way would have the same Hilbert space and the same terms as the model defined by Eq. (1) but would also have additional Heisenberg-type terms that couple the f electrons at different sites. In lowest order, such superexchange terms are of the form $\Sigma_{ij} J_{ij} \mathbf{S}_i \mathbf{S}_j$, where $\mathbf{S}_i \mathbf{S}_j = 1/2 \Sigma_{\sigma\sigma'} f_{i\sigma}^\dagger f_{i\sigma'} f_{j\sigma'}^\dagger f_{j\sigma}$ and J_{ij} is the intersite coupling generated by the removal of the double occupancy of the f states. In the PAM-Heisenberg model, J_{ij} is treated as a free parameter, and the limit $U=+\infty$ is taken with a nonvanishing J_{ij}. The mean-field SB solution of the $(U=+\infty)$ PAM-Heisenberg model should not be too different from the corresponding solution of the Kondo-Heisenberg model,[25–27] which gives the transition between the $r \neq 0$ and $r=0$ solutions when the superexchange energy exceeds some critical value of the order of Kondo energy. At the transition, both T_0 and T_K vanish continuously. Note that the relation between T_K and the physical observables would now have to be reconsidered because the decrease in the paramagnetic entropy [see Fig. 2] is not simply due to the onset of the Kondo effect but is also affected by the intersite magnetic fluctuations. The correct description of the critical properties should go beyond the mean-field approximation.[28]

H. Transport coefficients in the FL regime

The slave boson Hamiltonian in Eq. (3) can be used to define the approximate FL scale T_0 and the low-temperature thermodynamics but has no relaxation mechanisms that could lead to stationary heat and charge currents. To calculate the transport properties of the SU(N) symmetric Anderson model in the $T \to 0$ limit, we use the Fermi-liquid theory[29] which takes into account the QP damping and leads to a finite relaxation time. The QP excitations of the full model have the same dispersion as the excitations of the MF slave boson model but are restricted to the immediate vicinity of the Fermi level. In the $\omega \to 0$ limit, where the imaginary part of the f electron self-energy $\Sigma_f(\omega)$ can be neglected, the QP and the slave boson dispersion assume the same form. The correspondence is obtained by identifying rV with $\sqrt{Z_f}$ and λ with $\tilde{\omega}_f$, where $Z_f^{-1}=[1-\partial \Sigma_f/\partial \omega|_{\omega=0}]$ is the renormalization factor, $\tilde{\omega}_f=[E_f+\mathrm{Re}\,\Sigma_f(0)-\mu]Z_f$ is the renormalized position of the f level, and the excitation energies ω are measured in both cases with respect to the renormalized chemical potential μ. Unlike the infinitely long-lived MF excitations, which are formally defined for $\omega \leq D-\mu$, the QP excitations are defined for $\mathrm{Im}\,\Sigma_f(\omega) \ll \omega^2$.

We calculate the transport coefficients of the periodic Anderson model with constant hybridization using the fact that the charge and energy current density operators satisfy the Jonson-Mahan theorem.[30] This allows us to express the charge conductivity by $\sigma(T)=e^2 N L_{11}$, the thermopower by $\alpha(T)|e|T=-L_{12}/L_{11}$, and the electronic contribution to the thermal conductivity by $\kappa(T)T=N(L_{22}-L_{12}^2/L_{11})$. In each of these expressions, we have introduced the transport integrals

$$L_{mn} = \int d\omega \left(-\frac{dn_F}{d\omega} \right) \omega^{m+n-2} \Lambda(\omega, T). \tag{40}$$

where $n_F(\omega) = 1/[1+\exp(\beta\omega)]$ is the Fermi-Dirac distribution function and $\Lambda(\omega, T)$ is defined by the Kubo linear-response theory.[21] At low temperature $(-dn_F/d\omega)$ approaches delta function and the main contribution to the integrals in Eq. (40) comes from the low-energy excitations within the Fermi window $|\omega| \lesssim T$. In the ω, $T \to 0$ limit, a straightforward calculation yields for the three-dimensional systems[17]

$$\Lambda(\omega, T) = \tfrac{1}{3} v_F^2 \rho_c(\omega) \tau(\omega, T), \tag{41}$$

where we introduced the unrenormalized velocity $v_{\mathbf{k}} = -\nabla_{\mathbf{k}} \epsilon_{\mathbf{k}}$ and denoted by v_F^2 the average of $v_{\mathbf{k}}^2$ over the renormalized Fermi surface of hybridized states. The renormalized c DOS is $\rho_c(\omega)$ and the relaxation time is $1/\tau(\omega, T) \simeq \mathrm{Im}\, \Sigma_c(\omega)$, where $\Sigma_c(\omega)$ is the self-energy of the c electrons which must include the quasiparticle damping. The integrals in Eq. (40) are evaluated by the Sommerfeld expansion (for details see Ref. 17) which yields the transport coefficients of the periodic Anderson model as simple powers of reduced temperature T/T_0. The prefactors of various powers are functions of $\rho_0(\mu_L)$, n_f, and $\Delta\mu$ which depend on the local self-energy $\Sigma_f(\omega)$ which is difficult to obtain for the excitation energies within the Fermi window $|\omega| \leq T$. To avoid this problems, we replace T_0 and all other renormalized quantities that appear in the FL expressions by the slave boson MF results.

The FL result for the electrical resistivity can be written as[17]

$$R(T) \simeq \frac{9^2(\Delta\mu/n_f)^2}{N(N-1)\pi e^2 v_F^2} (\gamma T)^2 = \frac{9\pi^3(\Delta\mu/n_f)^2 T_K^2}{N(N-1)e^2 v_F^2 T_0^2} \left(\frac{T}{T_K} \right)^2 = AT^2, \tag{42}$$

where $\gamma = (\pi^2/6) N\rho(\mu) = \pi^2/3T_0$ and in the second equality $R(T)$ is expressed on the reduced temperature scale T/T_K. The coefficient $A = R(T)/T^2$ depends not only on specific-heat coefficient γ but on the difference in the chemical potentials of unhybridized and hybridized Bloch states, the effective degeneracy of the model, and the square of the Fermi velocity averaged over the hybridized FS. This result can be used to explain the pressure and magnetic field dependence of A, which has been studied experimentally in various systems.

The FL result for the Seebeck coefficient is given for $n_f \simeq 1$ by the expression

$$\alpha(T) = \mp \frac{12\gamma T}{n_f |e|} = \mp \frac{4\pi^2 T_K}{n_f |e| T_0} \frac{T}{T_K}. \tag{43}$$

Since the doubly occupied f states are removed from the Hilbert space, the model is highly asymmetric, and the initial slope $\lim_{T\to 0} \alpha(T)/T$ never vanishes. In bad metals with a low-carrier concentration, $\alpha(T)$ could be very large.

The thermal conductivity in the FL regime reads as

$$\kappa(T) = T\sigma(T)\mathcal{L}_0(T), \tag{44}$$

which yields in the $T \to 0$ limit the Wiedemann-Franz (WF) law $\kappa(T) \propto T\sigma(T)$. However, the usual Lorentz number $L_0 = \pi^2/3e^2$ is here replaced by the effective one,

$$\mathcal{L}_0(T) = \frac{\pi^2}{2e^2} \left[1 - \frac{32\pi^2}{n_f^2} \left(\frac{T}{T_0} \right)^2 \right]. \tag{45}$$

The correction given by the square bracket could lead to substantial deviations from the WF law much below T_0, since the factor multiplying the T^2 term is very large.

III. DISCUSSION OF THE EXPERIMENTAL DATA

The slave boson solution of the periodic Anderson model is used in this section to discuss the effects of the band structure on the properties of the intermetallic compounds with $4f$ ions. First, we consider the case of the c DOS with a maximum in the vicinity of the chemical potential such that the Fermi-liquid scale is much smaller than the Kondo scale $T_0 \ll T_K$. These results provide a qualitative explanation of the experiments on $YbAl_3$ or $YbMgAl_4$. The opposite case $T_0 \gg T_K$ occurs when the chemical potential is close to the minimum of the c DOS; these results explain the main experimental features of $YbInCu_4$-like compounds. Finally, for $T_0 \simeq T_K$, which seems to characterize $CeCu_2Si_2$ and $CeCu_2Ge_2$, we discuss the rapid variation in the T^2 coefficient of the electrical resistance and of the residual resistance with pressure. The anomalies are related to the pressure-induced change in the effective degeneracy of the f states.

A. $T_0 \ll T_K$ case

Unlike the experiments on dilute alloys, the overall temperature dependence of the experimental data on $YbAl_3$, $Yb_{1-x}Lu_xAl_3$ (Ref. 9) for $x \leq 0.05$, $YbMgCu_4$, and $YbCdCu_4$ (Ref. 31) cannot be explained by a single energy scale. In these compounds, the high-temperature resistivity is a large and slowly varying function of temperature,[32,33] the thermopower[32,33] has a broad peak around 350 K, the magnetic susceptibility and the specific heat have a broad maximum at $T_{\max} \simeq 125$ K, and the Hall coefficient is typical of a metal in which the c electrons scatter on local moments.[9,34] A similar high-temperature behavior is seen in $YbXCu_4$ ($X = \mathrm{Cd}, \mathrm{Mg}, \mathrm{Zn}$).[35] The inelastic neutron scattering data on $YbAl_3$ show a broad Lorentzian spectrum centered at about 540 meV,[36,37] which can be understood in terms of the Kondo effect with $T_K \geq 500$ K.[34] Below 100 K, the electrical resistivity of $YbAl_3$ decreases due to the formation of a coherent ground state and for $T \leq T_0 \simeq 40$ K the resistivity is a parabolic and the thermopower is a linear function of temperature,[32,33,38] indicating a Fermi liquid. For $T \leq T_0$, the zero-field anomalies in $\chi(T)$ and $C_V(T)$ yield an enhanced effective mass[34] of the order of $1/T_0$ and the neutron-scattering data[36,37] show a narrow peak at about 30 meV, which is due to a hybridization gap. However, if we plot the low-temperature transport coefficients on a reduced temperature scale T/T_K, they appear to be strongly enhanced with respect to the predictions of the single-impurity Anderson

model with Kondo scale $T_K \simeq 500$ K. Neither the A coefficient of the resistivity nor the slope of the thermopower can be explained by the single-impurity calculations that would capture the main features of the high-temperature data and give $T_K \simeq 500$ K. Optical conductivity at 7 K shows a narrow Drude-type response that is often found in heavy fermion systems[39,40] and another midinfrared peak (MIR) that can be associated with the hybridization gap. The optical spectra do not change appreciably for 7 K $\leq T \leq 40$ K, as expected of a system with the characteristic energy scale $T_0 \simeq 50$ K. However, the Drude peak broadens and the MIR peak vanishes at higher temperatures. The de Haas–van Alphen experiments performed up to $h \simeq 40$ T show that the effective mass is reduced along certain directions in **k** space by a factor of 2 without a significant alteration of the shape of the Fermi surface.[41] The fact that the low-temperature susceptibility anomaly is suppressed in the fields of about 40 T indicates that the high-field mass renormalization and the zero-field anomalies below T_0 describe different aspects of the same physical state. The low-temperature anomalies are easily destroyed by disorder (they vanish in $Yb_{1-x}Lu_xAl_3$ for $x \geq 0.05$), which is another indication that they are related to the coherent state.[41]

The overall shape of the experimental data and different characteristic energy scales found at high and low temperatures can be explained by the slave boson solution of the periodic Anderson model close to half-filling. As shown in Secs. II E and II F, if the chemical potential is close to the maximum of the unperturbed c DOS, the mean-field equations yield $T_0 \ll T_K \simeq h_c^0$ and give rise to a "slow crossover" from the LM to the FL phase. Taking $T_0 \simeq 50$ K and $T_K \simeq 500$, as suggested by the experiment, we find that the low-temperature susceptibility and the specific-heat coefficient are FL-like and much enhanced with respect to the expectations based on the behavior in the incoherent regime. The FL results for the T^2 term of the resistivity (see Sec. II H) explain the enhancement that one finds below 50 K when $\rho(T)$ is plotted on the T/T_K scale. The low-temperature thermopower $\alpha(T) \propto (T_K/T_0)T/T_K$ is also enhanced by T_K/T_0 with respect to the predictions of the single-impurity calculation that reproduce the thermopower maximum above 300 K. For temperatures between T_0 and T_K, the magnetization and the magnetic entropy are reduced with respect to the free-ion value, which is only recovered for $T > T_K$. The slave boson solution gives $m_z(h) \simeq h/T_0$ for $h \ll T_0$ and $m_z(h) \propto$ constant for $h \gg T_0$. Since $T_0 \ll h_c^0$, the slave boson order parameter is finite for $h \geq T_0$, i.e., for $T_0 \leq h \leq T_K$, the system is a polarized heavy FL with a "large FS." Such a behavior explains de Haas–van Alphen data which show that the FS does not change much up to the fields of about 40 T.

The model with the chemical potential close to the maximum in the c DOS describes $Yb_{1-x}Lu_xAl_3$ for $x \leq 0.5$. For higher concentrations of Lu, there are so many additional holes in the conduction band that the chemical potential shifts away from the peak in the c DOS. In that case, T_0 and T_K approach each other and the "slow" crossover does not occur. For $x > 0.5$, one can expect a crossover from a lattice regime with $T_0 \neq T_K$ to a universal dilute regime with $T_K = T_0$, as discussed in Ref. 42.

The slave boson dispersion defined by the Hamiltonian in Eq. (3) explains the Drude and the MIR peaks found at 7 K in the optical conductivity. However, we hesitate to discuss the temperature dependence of the hybridization gap using the mean-field results. These results are obtained by enforcing the constraint $n_f = 1$ only on the average, so that the auxiliary fermions are mapped on a free-electron gas. The proper redistribution of the spectral weight should not neglect the QP damping and should use the solution which is valid at all energy scales.

B. $T_0 \gg T_K$ case

In $Yb_{1-x}Lu_xAl_3$ for $x \geq 0.7$, $YbTlCu_4$,[31] $YbInCu_4$, and $Yb_{1-x}Y_xInCu_4$ for $x \leq 0.5$,[10] unlike in $YbAl_3$ or $Yb_{1-x}Lu_xAl_3$ for $x \leq 0.5$, the transition between the LM and the FL phase occurs in an abrupt way. In $YbInCu_4$, which we take as a typical example, the transition occurs at ambient pressure at temperature $T_v = 40$ K, where a first-order valence (VF) change takes place. Above T_v, the Yb ions are in the 3^+ configuration and the magnetic response can be understood assuming an independent $4f$ hole in each unit cell. The ensuing high-temperature effective moment is then close to the free ion value, as observed experimentally.[10] The electrical resistance is very large and nearly temperature independent.[43] The Kondo scale deduced from these data is so much smaller than T_v that the f and c states are effectively decoupled for $T \geq T_v$. The magnetic fields up to 40 T do not produce any appreciable magnetoresistance which is also an indication of a small Kondo coupling. A large (constant) electrical resistance[43] and a very small Hall constant[44] cannot be explained in terms of the spin-disorder scattering but can be taken as evidence[44,45] that the unperturbed c DOS has a pseudogap or a deep minimum in the vicinity of the chemical potential. When the compound is cooled down to temperature T_v, the lattice expands and the Yb configuration changes from 3^+ to 2.9^+. In the VF phase, the susceptibility and the specific-heat coefficient are moderately enhanced ($\gamma \simeq 50$ mJ/mol K), the resistivity is quadratic, and the thermopower is linear in temperature. The ratio $\alpha/T\gamma$ is typical of a normal FL (Ref. 46) but the Kadowaki-Woods ratio is anomalously low. The characteristic energy scale in the VF phase is much larger than T_v; the data give $T_0 \simeq 500$ K.[47] The optical conductivity,[48] the Hall effect,[44] and the thermoelectric power[49] indicate that a bad metal with only a few states close to the chemical potential is transformed at T_v into a good metal with small γ. That is, the VF transition is accompanied by a major reconstruction of the conduction states.

An application of pressure shifts $T_v(P)$ to lower temperatures[50–53] without changing the properties of the high-temperature state. For $T \geq T_v(P)$, the susceptibility and the specific heat of $YbInCu_4$ can be explained by the CF theory of independent f states[54] split by $\Delta_{CF} \simeq 40$ K into an excited quartet and two nearly degenerate doublets. This CF scheme agrees with the neutron-scattering data.[55] The entropy of the LM phase obtained by integrating $C_V(T)/T$ (Refs. 52 and 54) decreases from $S \simeq R \ln 8$ to $S \simeq R \ln 4$ as the system is cooled down to $T_v(P)$, as expected for two CF quartets without any Kondo screening. This indicates, once again, that the Kondo scale of the LM phase is much smaller

than $T_v(P)$. Pressure stabilizes the paramagnetic phase and at a critical pressure of $P_c=2.5$ GPa the LM persists down to $T_c=2.5$ K, where the magnetic transition removes the paramagnetic entropy of about $S\simeq R\ln 4$. The NMR (Refs. 50 and 53) and neutron-scattering data show that the local moments in the magnetically ordered (MO) phase are somewhat smaller than in the LM phase just above T_N. Since the specific-heat coefficient and the A coefficient of the resistivity are much larger for $P\geq P_c$ than for $P\leq P_c$, we speculate that the transition in the MO phase is accompanied by an increase in Kondo coupling. As regards the doping, replacing Yb with Y or Lu ions[51,56] produces similar effects as pressure, i.e., doping stabilizes the LM configuration and shifts T_c to lower temperatures. In Eu-based intermetallics, the valence-change transition exhibits similar features[11,12] as in $YbInCu_4$, except T_v is higher ($T_v\geq 100$ K) and the valence state of Eu ions changes almost completely [from 2^+ (f^7) to 3^+ (f^6)].

We close this experimental summary by mentioning that the VF transition shifts in a magnetic field to lower temperatures. At ambient pressure, the critical field of $h_c^0\simeq 40$ T suppresses the VF transition and removes completely the FL state of $YbInCu_4$. The experiments give $\mu_{\rm eff}h_c^0=T_v$, where $\mu_{\rm eff}$ is the effective magnetization of the $4f$ state in the LM regime, i.e., at the VF transition, the magnetic energy of the paramagnetic f states is comparable to the Kondo energy of the FL phase. The critical field is temperature dependent and the phase boundary between the LM phase and the FL phase is given by the expression $h_c(T)=h_c^0\sqrt{1-(T/T_v)^2}$, where h_c^0 is the zero-temperature value.

The aforementioned behavior of $YbInCu_4$ and similar systems can be understood from the slave boson solution of the periodic Anderson model by assuming that the chemical potential of the high-temperature phase is close to the pseudogap of the unrenormalized c DOS, as suggested by the experimental data[44] and the band-structure calculations.[45] The results presented in Sec. II C give then a very small Kondo temperature which explains the Curie-type susceptibility, a large and nearly temperature-independent resistivity, small thermopower, and a negligible magnetoresistance observed in these systems above the valence-change transition. Since the Kondo screening is absent in the LM phase, we can neglect the hybridization altogether and discuss the high-temperature properties of $YbInCu_4$ by adding the Falicov-Kimball term to the effective Hamiltonian. This term stabilizes the gap or a pseudogap in the excitation spectrum[57] and explains most of the qualitative features in a self-consistent way. For a quantitative description of the paramagnetic phase, one would have to include the corrections due to the CF splitting of the f states.[58]

The peculiar feature of $YbInCu_4$-like systems is that the local moments remain unscreened down to very low temperatures. Because of the pseudogap in the c DOS, the system cannot remove the paramagnetic entropy by Kondo effect but has to approach the ground state by an entirely different route. In $YbInCu_4$, the transition into a low-entropy state is achieved by an isostructural phase transition which expands the lattice and facilitates the valence fluctuations between the low-volume $4f^{13}$ and the large-volume $4f^{14}$ states of Yb. The presence of the $4f^{14}$ configuration in the ground state means that some f holes are transferred in the c band. This moves the chemical potential out of the pseudogap region, increases the Kondo coupling, and makes the Kondo temperature of the expanded lattice comparable to T_v. For $T\leq T_v$, the local moment disappears because the f and c states form hybridized bands. The increase in the Kondo coupling and the lattice expansion terminate when the Kondo scale of the hybridized system becomes equal to T_v, as can be seen from the following argument. At T_v, the free energy of the high-temperature (local moment) phase and the low-temperature (FL) phase are equal $\mathcal{F}_{\rm LM}=\mathcal{F}_{\rm FL}$, i.e., the energy gain due to hybridization compensates the loss of magnetic entropy and a small loss of elastic energy due to lattice expansion. Below T_v, the free energy is dominated by the hybridization term in the internal energy which stabilizes the (low-entropy) FL state, such that $|\Delta E|\geq T\Delta S$ and $\mathcal{F}_{\rm FL}<\mathcal{F}_{\rm LM}$. If we assume $T_K\leq T_v$, then, by definition of T_K, the system with finite Kondo coupling would be paramagnetic for $T_K\leq T\leq T_v$ but the f moments would still be partially screened. The magnetic entropy of such an expanded system is smaller than the entropy of the pseudogapped phase with completely free local moments. Thus, for $T\leq T_v$, the magnetic entropy of partly screened local moments is too small to destabilize the FL state and we conclude that T_K of the expanded lattice with hybridized states cannot be smaller than T_v.

In the expanded lattice, the chemical potential is still rather close to the minimum of the c DOS, which makes the FL scale much larger than the Kondo scale T_v (see Sec. II D). If we estimate the FL corrections to the $T=0$ value of the magnetic susceptibility or the electric resistivity up to $\mathcal{O}[(T/T_0)^2]$ and assume $T_0/T_K\leq 10$ (as indicated by the data), the maximum relative deviation at $T\sim T_v$ is 1%. The Kadowaki-Woods ratio in the FL phase is anomalously small because the CF splitting does not affect the delocalized f states, so that the f states are effectively eightfold degenerate. The FL analysis presented in Sec. III and III shows that the A coefficient is then reduced by a factor $1/N(N-1)$. Thus, the slave boson theory provides an overall description of $YbInCu_4$-like compounds at ambient pressure.

To explain the pressure effects, we recall that pressure stabilizes the low-volume ($4f^{13}$) configuration with respect to the large-volume ($4f^{14}$) one and we take this into account by shifting the f level away from the chemical potential. This reduces the f-c coupling and the Kondo scale shifts T_v to lower temperatures and removes eventually the VF transition. For very large pressures, the paramagnetic entropy of the LM phase is not removed by the lattice expansion but by a transition into a MO phase which takes place at Curie temperature T_c.

In the presence of an external magnetic field, the condition for the phase boundary $\mathcal{F}_{\rm LM}(T,h)=\mathcal{F}_{\rm FL}(T,h)$ can be approximated by the condition $S_{\rm LM}(T_v,h)=$const, where $S_{\rm LM}(T_v,h)$ is the entropy of the LM phase.[59] This approximation uses the fact that T_0 is not affected by the pseudogap, so that $T_0\gg T_v$, and the temperature and the field dependence of $\mathcal{F}_{\rm FL}$ can be neglected for $T\leq T_v(h)$. The critical line obtained in such a way agrees very well with the experimental data[58,60] and with the slave boson result given by Eq. (39). For large fields, the slave boson solution shown by the

dashed-dotted curve in Fig. 5 explains the metamagnetic transition that takes place at the critical field $h_c^0 \propto T_v$.

Similar reasoning explains also the unusual behavior of the newly reported system Yb_3Pt_4.[61,62] In the paramagnetic phase, Yb_3Pt_4 has the Curie-type susceptibility and nearly constant resistivity which exceeds the spin-disorder limit. Like in $YbInCu_4$, the LM phase of Yb_3Pt_4 looks semimetallic, with unrenormalized ("light") Bloch sates and localized f states. In the absence of the f-c exchange coupling, the paramagnetic entropy cannot be reduced by the Kondo screening but the ground state has to be approached by an alternative route. In Yb_3Pt_4, the ground state is magnetic and we speculate that the LRO is due to a spin-density wave (SDW). The transition between the LM and the SDW phase takes place at $T_N \simeq 2$ K. The data show that the effective mass of metallic electrons becomes heavy at T_N.[62]

This behavior can be explained by the slave boson approach, assuming that the chemical potential is close to the pseudogap of the unperturbed c band and admitting an antiferromagnetic (AFM) solution. The generalized slave boson equations which include the coupling to the staggered magnetization provide at T_N a nontrivial solution with hybridized states and a large FS. The reason is that large internal fields shift the chemical potential of up and down spins away from the singularity in c DOS (like in the case of an external magnetic field discussed in Sec. II F). Since the Kondo coupling in the LM phase is very small, the c electrons are nearly free and the Kondo screening can only occur at extremely low temperatures. Unlike $YbInCu_4$, where the paramagnetic entropy is removed by an isostructural phase transition which enables hybridization and the transition to the FL phase, in Yb_3Pt_4 the paramagnetic entropy is removed by a SDW transition which partially gaps the Fermi surface. The formation of the SDW at temperature $T_N \simeq 2$ K switches on the hybridization, which delocalizes the f states, changes the effective degeneracy of the f states, and renormalizes the metallic mass. The chemical potential in the SDW phase is still rather close to the pseudogap, so that the ensuing FL scale is large $T_0 \gg T_N$ (see discussion in Sec. II D). Hence, the mass enhancement at the transition is moderate or small. It would be interesting to check the assumption about the pseudogap in the c DOS by performing the band-structure calculations that would take into account the large Coulomb repulsion between the f electrons.

C. $T_0 \simeq T_K$ case

As a final example, we consider the anomalous pressure dependence of the T^2 coefficient of the resistivity $A(P)$ and the residual resistance $\rho_0(P)$ observed in heavy fermions such as $CeCu_2Si_2$,[63] $CeCu_2Ge_2$,[64] or $CePd_2Ge_2$ (Ref. 65) at very low temperatures. In these compounds, the FL scale is about the same as the Kondo scale inferred from the low-temperature peak in $\rho(T)$ or $\alpha(T)$.[17,64] The scales T_0 and T_K are much smaller than the CF splitting [estimated from the high-temperature peak in $\rho(T)$ or $\alpha(T)$ (Ref. 17)], so that the excited CF sates can be neglected for $T \leq T_K \ll \Delta_{\mathrm{CF}}$. At ambient pressure, the ground state of these compounds is often superconducting or magnetic and the FL behavior is enforced by applying an initial pressure P_0. For $P > P_0$, the data show that $A(P)$ decreases gradually from large initial values, drops at a critical pressure P_c by nearly 2 orders of magnitude,[63–65] and then continues a gradual decrease. The residual resistance increases from a small initial value, rises rapidly to a sharp peak at P_c, and decreases at very high pressure to rather small values.[63,64]

We explain these features by assuming that for $P_0 \leq P \leq P_c$, the effective degeneracy of the model is defined by the lowest CF state and that pressure changes the f-c coupling and T_K but not Δ_{CF}. The FL state established at P_0 has a large Fermi surface because the f electrons are delocalized and participate in the Fermi sea. Taking, for simplicity, the half-filled conduction band and describing the $4f$ state be a CF doublet, we find that the Fermi surface is close to the edge of the Brillouin zone and that the average Fermi velocity in Eq. (42) is small. In the aforementioned compounds, the FL scale is also small so that $A(P_0)$ is large. As long as pressure does not change the degeneracy of the f states, Luttinger theorem preserves the Fermi surface, so that v_F^2 and $\Delta\mu$ in Eq. (42) remain approximately constant. Since N is also constant in this pressure range, the prefactor of the $(\gamma T)^2$ term in Eq. (42) does not change much. Thus, the main effect of pressure is a gradual reduction of $A(P)$ from the maximum value attained at P_0. This reduction is due to the increase of $T_0(P)$, as can be seen from the linear scaling between $\sqrt{A(P)}$ and the inverse Kondo scale of the system $1/T_K(P)$.[64]

At large enough pressure, the hybridization becomes too large for the system to support the CF excitations, so that the effective degeneracy of the ground state increases. For $P \geq P_c$, the degeneracy is not set any more by the lowest CF level but by the full multiplet (a sextet, in the case of Cerium). The slave boson solution of the periodic Anderson model with the SU(N) symmetry and infinite correlation shows that the Fermi volume decreases as N increases because a single f electron is distributed over more and more equivalent channels. The chemical shift $\Delta\mu$ and the specific-heat coefficient γ also decrease with N, while v_F^2 is larger for a smaller FS. Thus, $A(P)$ drops sharply for $P \geq P_c$. The degeneracy of the f state cannot increase above $N=6$ for Ce and $N=8$ for Yb, so that an increase in pressure above P_c can only reduce $A(P)$ by increasing T_0. In this pressure range, we find the scaling between $\sqrt{A(P)}$ and the inverse Kondo scale of the N-fold degenerate model which is much bigger than T_K. Note that the periodic Anderson model with infinite f-f correlation, as defined by Eq. (3), cannot describe the enhancement of the A coefficient due to the intersite magnetic fluctuations.

The residual resistance also tracks the pressure-induced changes in the effective degeneracy. If the f states are localized at ambient pressure, as seems to be the case with $CeCu_2Ge_2$ (Ref. 64) or $CePd_2Ge_2$ (Ref. 65) at very low temperatures, the initial values of $\rho_0(P_0)$ are small. Taking, for simplicity, the model with a ground-state doublet and an excited CF quartet and using the FL laws, we find that the temperature dependence of the resistivity at ambient pressure is due to two resonant channels; while most of the current is carried by four nonresonant channels which have temperature-independent conductivity. The contribution of the resonant channels to the residual resistance can be ne-

glected. At large enough pressure $P \simeq P_c$, the CF excitations are removed, the degeneracy of the ground state changes from doublet to sextet, and all the channels become resonant. Because of Luttinger theorem, the Fermi volume shrinks for two of the channels (former resonant ones) and expands for four of them (former nonresonant ones). Hence, for $P \simeq P_c$, the overall contribution to the residual resistance increases sharply. A further increase in pressure does not change the degeneracy of the model but gives rise to the charge transfer from the f to the c states. This reduces the residual resistance and gives the $\rho_0(P)$ curve its asymmetric shape. In other words, the FL liquid laws and the slave boson solution of the periodic Anderson model show that the large peaks in $A(P)$ and $\rho_0(P)$ are due to the pressure-induced change in the degeneracy of the f state.

IV. SUMMARY AND CONCLUSIONS

It is well known that the degeneracies and the splittings of the $4f$ states have a strong impact on the Kondo scale and the high-temperature behavior of intermetallic compounds with Ce, Eu, or Yb ions. In this paper, we have shown that the details of the conduction-electron band structure have a large impact on the ratio of the Kondo scale to the Fermi liquid scale, which determines the type of the crossover between the incoherent and coherent regimes.

Our analysis is based on the periodic Anderson model with infinite intrasite f-f correlation. At high temperatures, this model can be mapped on a single-impurity Anderson or Kondo model with Kondo scale T_K and its incoherent properties can be obtained from the single-impurity approximations that take into account the structure of the f and c states. At low temperatures, where the coherent behavior sets in, the slave boson solution yields the FL laws characterized by an energy scale T_0. The Kondo and the FL scales depend on the shape of the c DOS in the vicinity of the chemical potential, the degeneracy and the CF splitting of the f states, the number of c and f electrons, and their coupling. Our calculations show that the ratio T_0/T_K is determined by the details of the band structure. Depending on the relative magnitude of T_0 and T_K, the crossover between the high- and low-temperature regimes proceeds along very different routes. A sharp peak in the c DOS yields $T_0 \ll T_K$ and gives rise to a "slow crossover," as observed in $YbAl_3$ and similar compounds. The minimum in the c DOS yields $T_0 \gg T_K$, which causes an abrupt transition between the high- and low-temperature regimes, as observed in $YbInCu_4$-like systems. In the case of $CeCu_2Ge_2$ and $CeCu_2Si_2$, where $T_0 \simeq T_K$, our results show that the pressure dependence of the $A(P)$ coefficient and the residual resistance can be related to the change in the degeneracy of the f states.

The slave boson solution shows that the low-temperature response of the periodic model can be enhanced (or reduced) with respect to the predictions of the single-impurity model with the same Kondo scale. In the coherent regime, the renormalization of transport coefficients modifies the Wiedemann-Franz law and can lead to an enhancement of the thermoelectric figure of merit. The FL laws explain the correlation between the specific-heat coefficient γ and the slope of the thermopower $\alpha(T)/T$ or between γ and the T^2 coefficient of the electrical resistance $A=\rho(T)/T^2$. In the case of an N-fold degenerate model, the FL laws explain the deviations of the Kadowaki-Woods ratio $R_{\mathrm{KW}}=A/\gamma^2$ and the q ratio $q=|e|\lim_{\{T\to 0\}x}\alpha/\gamma T$ from the universal values.

The magnetic response is also affected by the shape of the c DOS. The field dependence of the magnetization given by the SB solution resembles the temperature dependence of the entropy, as can be seen from Figs. 5 and 2. The c DOS with a maximum around the chemical potential leads to an extended plateau in $m(h)$, while a pseudogap in the c DOS leads to a metamagnetic transition for the fields on the order of the Kondo temperature.

Before closing, we mention that the intersite magnetic fluctuations are completely neglected in the Hamiltonian given by Eq. (3). The localized boson that we introduced to solve the model is associated with the $4f^0$ configuration and its condensation marks the formation of a hybridized FL state. Neither the magnetic transitions nor the competition between the Kondo effect and magnetism can be described by the simple model with infinite intrasite f-f correlation. The intersite effects can be described by generalizing the model, so as to add the Heisenber-type terms to Eq. (1). We believe that the SB treatment of such an infinite-U PAM-Heisenberg model could provide an insight into pressure experiments in which the number of f electrons changes as one approaches the magnetic boundary.

ACKNOWLEDGMENTS

The authors are grateful to R. Monnier, J. Freericks, and M. Vojta for useful discussions. S.B. acknowledges the Max Planck Institute for the Physics of Complex Systems, Dresden, Germany, where part of this work has been done. V.Z. acknowledges the hospitality of the Aspen Center for Physics where part of this work has been done. Support from the Ministry of Science of Croatia under Grant No. 0035-0352843-2849, from the NSF under Grant No. DMR-0210717, and from the COST P-16 ECOM project are acknowledged. A part of this work was funded by the DFG through Grants No. SFB 680, No. SFB/TR 12, and No. FG 960.

APPENDIX A: GENERALIZATION TO MULTIORBITAL SYSTEMS

1. General formalism

We generalize our model by allowing the local f orbital to have a supplementary degeneracy. The latter is lifted at low temperature by the crystalline electrical field. In the limit $U\to\infty$, the PAM Hamiltonian (1) generalized in such a way reads as

$$H=\sum_{\mathbf{k}\sigma}\epsilon_{\mathbf{k}}c^{\dagger}_{\mathbf{k}\sigma}c_{\mathbf{k}\sigma}+\sum_{i\alpha\sigma}(E_f+\Delta^{\alpha}_{\mathrm{CF}})f^{\dagger}_{i\alpha\sigma}f_{i\alpha\sigma}+V\sum_{i\alpha\sigma}[c^{\dagger}_{i\sigma}f_{i\alpha\sigma}+f^{\dagger}_{i\alpha\sigma}c_{i\sigma}]-\mu\sum_{i\sigma}\left[\sum_{\alpha}f^{\dagger}_{i\alpha\sigma}f_{i\alpha\sigma}+c^{\dagger}_{i\sigma}c_{i\sigma}\right], \tag{A1}$$

where $\alpha=1,\ldots,N/2$ is a local orbital index, and $\Delta^{\alpha}_{\mathrm{CF}}$ defines

the crystal-field splitting. For Ce and Yb, we have $N=6$ and $N=8$. The slave boson approach described in Sec. II for $N=2$ is defined by the mapping $|0\rangle_i^f \to b_i^\dagger|0\rangle_i$, $|\alpha\sigma\rangle_i^f \to d_{i\alpha\sigma}^\dagger|0\rangle_i$, and by excluding all the states with more than one electron on a given site. This leads to the local identities $b_i^\dagger b_i + \Sigma_{\alpha\sigma} f_{i\alpha\sigma}^\dagger f_{i\alpha\sigma} = 1$, which are satisfied by introducing Lagrange multipliers λ_i. Within the mean-field approximation, we replace the bosonic fields b_i and the Lagrange multipliers λ_i by homogeneous static real fields r and λ. The quadratic mean-field Hamiltonian (3) obtained for $N=2$ is then generalized to

$$H = \sum_{\mathbf{k}\sigma} \left[\epsilon_{\mathbf{k}} c_{\mathbf{k}\sigma}^\dagger c_{\mathbf{k}\sigma} + rV \sum_\alpha (c_{\mathbf{k}\sigma}^\dagger d_{\mathbf{k}\alpha\sigma} + d_{\mathbf{k}\alpha\sigma}^\dagger c_{\mathbf{k}\sigma}) - \mu c_{\mathbf{k}\sigma}^\dagger c_{\mathbf{k}\sigma} + \sum_\alpha (\lambda + \Delta_{\mathrm{CF}}^\alpha) d_{\mathbf{k}\alpha\sigma}^\dagger d_{\mathbf{k}\alpha\sigma} + \frac{E_f - \lambda - \mu}{2}(1 - r^2) \right]. \quad \text{(A2)}$$

The self-consistent parameters r and λ are obtained by minimizing the free energy $\beta\mathcal{F}(r,\lambda) \equiv -\ln \mathrm{Tr} e^{-\beta H}$ such that $\partial\mathcal{F}(r,\lambda)/\partial r = 0$ and $\partial\mathcal{F}(r,\lambda)/\partial\lambda = 0$. This gives

$$2r(E_f - \lambda - \mu) = V \sum_{\mathbf{k}\alpha\sigma} \langle c_{\mathbf{k}\sigma}^\dagger d_{\mathbf{k}\alpha\sigma} + d_{\mathbf{k}\alpha\sigma}^\dagger c_{\mathbf{k}\sigma} \rangle, \quad \text{(A3)}$$

$$r^2 = 1 - \sum_{\mathbf{k}\alpha\sigma} \langle d_{\mathbf{k}\alpha\sigma}^\dagger d_{\mathbf{k}\alpha\sigma} \rangle, \quad \text{(A4)}$$

where, $\langle \cdots \rangle$ denotes the thermal average with respect to the mean-field Hamiltonian (A2) and we have

$$n = \sum_{i\sigma} \left\langle \sum_\alpha d_{i\alpha\sigma}^\dagger d_{i\alpha\sigma} + c_{i\sigma}^\dagger c_{i\sigma} \right\rangle \equiv \sum_\alpha n_f^\alpha + n_c. \quad \text{(A5)}$$

The average electronic occupation per site of the f and c orbitals is $n_f^\alpha \equiv \Sigma_{i\sigma} \langle f_{i\alpha\sigma}^\dagger f_{i\alpha\sigma} \rangle = \Sigma_{i\sigma} \langle d_{i\alpha\sigma}^\dagger d_{i\alpha\sigma} \rangle$ and $n_c \equiv \Sigma_{i\sigma} \langle c_{i\sigma}^\dagger c_{i\sigma} \rangle$, respectively. These averages are determined by the slave boson amplitude and the total electronic occupation,

$$\sum_\alpha n_f^\alpha = 1 - r^2, \quad \text{(A6)}$$

$$n_c = n - \sum_\alpha n_f^\alpha. \quad \text{(A7)}$$

The self-consistent Eqs. (A3)–(A5) can be rewritten as

$$r\frac{E_f - \lambda - \mu}{2} = -V \int_{-\infty}^{+\infty} \rho_{dc}(\omega) n_F(\omega) d\omega, \quad \text{(A8)}$$

$$\frac{n_f^\alpha}{2} = \int_{-\infty}^{+\infty} \rho_d^\alpha(\omega) n_F(\omega) d\omega, \quad \text{(A9)}$$

$$\frac{n_c}{2} = \int_{-\infty}^{+\infty} \rho_c(\omega) n_F(\omega) d\omega, \quad \text{(A10)}$$

where $n_F(\omega) \equiv 1/[1 + e^{\beta\omega}]$ is the Fermi function and ρ_{dc}, ρ_d^α, and ρ_c are the spectral densities of the local single-particle Green's functions of a given spin. These Green's functions are defined in the usual way as thermal averages of the (imaginary) time-ordered products of the appropriate creation and annihilation operators,

$$\rho_{dc}(\omega) \equiv -\frac{1}{\pi} \sum_{\mathbf{k}} \sum_\alpha \mathrm{Im}\, G_{dc}^\alpha(\mathbf{k},\omega), \quad \text{(A11)}$$

$$\rho_d^\alpha(\omega) \equiv -\frac{1}{\pi} \sum_{\mathbf{k}} \mathrm{Im}\, G_d^\alpha(\mathbf{k},\omega), \quad \text{(A12)}$$

$$\rho_c(\omega) \equiv -\frac{1}{\pi} \sum_{\mathbf{k}} \mathrm{Im}\, G_c(\mathbf{k},\omega). \quad \text{(A13)}$$

For the quadratic Hamiltonian (A2), the Green's functions are given by the expressions

$$G_{cc}(\mathbf{k},\omega) = \frac{1}{\omega + \mu - \epsilon_{\mathbf{k}} - r^2 V^2 \sum_\alpha 1/(\omega - \lambda - \Delta_{\mathrm{CF}}^\alpha)}, \quad \text{(A14)}$$

$$G_{dc}^\alpha(\mathbf{k},\omega) = -\frac{rV}{\omega - \lambda - \Delta_{\mathrm{CF}}^\alpha} G_{cc}(\mathbf{k},\omega), \quad \text{(A15)}$$

$$G_{dd}^\alpha(\mathbf{k},\omega) = \frac{1}{\omega - \lambda - \Delta_{\mathrm{CF}}^\alpha} + \frac{r^2 V^2}{(\omega - \lambda - \Delta_{\mathrm{CF}}^\alpha)^2} G_{cc}(\mathbf{k},\omega). \quad \text{(A16)}$$

Defining the noninteracting electron Green's function

$$G_0(\omega) \equiv \sum_{\mathbf{k}} \frac{1}{\omega - \epsilon_{\mathbf{k}}}, \quad \text{(A17)}$$

we can rewrite the local spectral densities as

$$\rho_c(\omega) = -\frac{1}{\pi} \mathrm{Im}\, G_0\left(\omega + \mu - r^2 V^2 \sum_\alpha \frac{1}{\omega - \lambda - \Delta_{\mathrm{CF}}^\alpha} \right), \quad \text{(A18)}$$

$$\rho_{dc}^\alpha(\omega) = \frac{1}{\pi} \mathrm{Im} \left[\frac{rV}{\omega - \lambda - \Delta_{\mathrm{CF}}^\alpha} \times G_0\left(\omega + \mu - r^2 V^2 \sum_\alpha \frac{1}{\omega - \lambda - \Delta_{\mathrm{CF}}^\alpha} \right) \right], \quad \text{(A19)}$$

$$\rho_d^\alpha(\omega) = -\frac{1}{\pi} \mathrm{Im} \left[\frac{1}{\omega - \lambda - \Delta_{\mathrm{CF}}^\alpha} + \frac{r^2 V^2}{(\omega - \lambda - \Delta_{\mathrm{CF}}^\alpha)^2} \times G_0\left(\omega + \mu - r^2 V^2 \sum_\alpha \frac{1}{\omega - \lambda - \Delta_{\mathrm{CF}}^\alpha} \right) \right]. \quad \text{(A20)}$$

2. Degenerate case: No crystal-field splitting

In the case $\Delta_{\mathrm{CF}}^\alpha = 0$, one can check easily that the complete formalism described in this paper for $N=2$ can be general-

ized to any value of N by making the transformation

$$V^2 \to \frac{N}{2} V^2. \tag{A21}$$

Due to the exponential dependence of T_0 and T_K on V^2 [see Eqs. (20), (22), and (34)], these characteristic energies have to be rescaled as

$$T_K^{(N)} = T_K^{(2)} e^{-(2-N)/NJ(\mu_0)\rho_0(\mu_0)}, \tag{A22}$$

$$T_0^{(N)} = T_0^{(2)} e^{-(2-N)/NJ(\mu_0)\rho_0(\mu_0)}, \tag{A23}$$

where N denotes the number of degenerate f channels.

3. Kondo temperature

For $r \to 0$, we write the generalized mean-field equations as

$$\frac{n_c}{2} = \int_{-\infty}^{+\infty} \rho_0(\omega+\mu) n_F(\omega) d\omega, \tag{A24}$$

$$\frac{n_c^\alpha}{2} = n_F(\lambda + \Delta_{\mathrm{CF}}^\alpha), \tag{A25}$$

$$\frac{E_f - \lambda - \mu}{V^2} = \sum_{\alpha=1}^{N/2} \int_{-\infty}^{+\infty} \frac{1}{\omega - \lambda - \Delta_{\mathrm{CF}}^\alpha} \rho_0(\omega+\mu) \tanh\left(\frac{\omega}{2T}\right) d\omega \tag{A26}$$

and set $\Delta_{\mathrm{CF}}^{\alpha=0}=0$ for the doublet with the lowest local energy E_f. At low enough temperatures, we have $\Delta_{\mathrm{CF}}^{\alpha\neq 0} \gg T$ for the excited doublets, which gives $n_f^{\alpha\neq 0} \approx 0$ and allows us to use the formalism developed for $N=2$ without any changes. At higher temperatures, such that $\Delta_{\mathrm{CF}}^{\alpha\neq 0} \sim T$ or $\Delta_{\mathrm{CF}}^{\alpha\neq 0} < T$, one also has to consider the contribution from the excited orbitals.

[1] P. W. Anderson, J. Phys. C **3**, 2346 (1970).
[2] K. G. Wilson, Rev. Mod. Phys. **47**, 773 (1975).
[3] P. Nozières, J. Low Temp. Phys. **17**, 31 (1974).
[4] K. Yamada, Prog. Theor. Phys. **53**, 970 (1975).
[5] A. Tsvelick and P. Wiegmann, Adv. Phys. **32**, 453 (1983).
[6] D. Withoff and E. Fradkin, Phys. Rev. Lett. **64**, 1835 (1990).
[7] M. Vojta and R. Bulla, Phys. Rev. B **65**, 014511 (2001).
[8] D. E. Sheehy and J. Schmalian, Phys. Rev. B **77**, 125129 (2008).
[9] E. D. Bauer, C. H. Booth, J. M. Lawrence, M. F. Hundley, J. L. Sarrao, J. D. Thompson, P. S. Riseborough, and T. Ebihara, Phys. Rev. B **69**, 125102 (2004).
[10] J. L. Sarrao, Physica B **259-261**, 128 (1999).
[11] H. Wada, A. Nakamura, A. Mitsuda, M. Shiga, T. Tanaka, H. Mitamura, and T. Goto, J. Phys.: Condens. Matter **9**, 7913 (1997).
[12] A. Mitsuda, H. Wada, M. Shiga, and T. Tanaka, J. Phys.: Condens. Matter **12**, 5287 (2000).
[13] S. Barnes, J. Phys. F: Met. Phys. **6**, 1375 (1976).
[14] P. Coleman, Phys. Rev. B **29**, 3035 (1984).
[15] V. Zlatić, R. Monnier, J. Freericks, and K. W. Becker, Phys. Rev. B **76**, 085122 (2007).
[16] S. Burdin, A. Georges, and D. R. Grempel, Phys. Rev. Lett. **85**, 1048 (2000).
[17] V. Zlatic, R. Monnier, and J. K. Freericks, Phys. Rev. B **78**, 045113 (2008).
[18] A. N. Tahvildar-Zadeh, M. Jarrell, and J. K. Freericks, Phys. Rev. B **55**, R3332 (1997).
[19] P. Nozières, Ann. Phys. (Paris) **10**, 19 (1985).
[20] P. Nozières, Eur. Phys. J. B **6**, 447 (1998).
[21] G. D. Mahan, *Many-Particle Physics* (Plenum, New York, 1981).
[22] S. Doniach, Physica **91**, 231 (1977).
[23] P. Coleman, Phys. Rev. B **28**, 5255 (1983).
[24] N. Read, D. M. Newns, and S. Doniach, Phys. Rev. B **30**, 3841 (1984).
[25] A. M. Sengupta and A. Georges, Phys. Rev. B **52**, 10295 (1995).
[26] J. R. Iglesias, C. Lacroix, and B. Coqblin, Phys. Rev. B **56**, 11820 (1997).
[27] S. Burdin, D. R. Grempel, and A. Georges, Phys. Rev. B **66**, 045111 (2002).
[28] I. Paul, C. Pepin, and M. R. Norman, Phys. Rev. Lett. **98**, 026402 (2007).
[29] K. Yamada and K. Yosida, Prog. Theor. Phys. **76**, 681 (1986).
[30] G. D. Mahan, in *Good Thermoelectrics*, Solid State Physics, edited by H. Ehrenreich and F. Spaepen (Academic Press, San Diego, 1997), Vol. 51, p. 81.
[31] J. M. Lawrence, P. S. Riseborough, C. H. Booth, J. L. Sarrao, J. D. Thompson, and R. Osborn, Phys. Rev. B **63**, 054427 (2001).
[32] H. J. van Daal, P. B. van Aken, and K. H. J. Buschow, Phys. Lett. **49**, 246 (1974).
[33] M. Rowe, V. L. Kuznetsov, L. A. Kuznetsova, and G. Min, J. Phys. D **35**, 2183 (2002).
[34] A. Cornelius *et al.*, Phys. Rev. Lett. **88**, 117201 (2002).
[35] J. M. Lawrence, P. S. Riseborough, C. H. Booth, J. L. Sarrao, J. D. Thompson, and R. Osborn, Phys. Rev. B **63**, 054427 (2001).
[36] A. P. Murani, Phys. Rev. Lett. **54**, 1444 (1985).
[37] R. Osborn, E. Goremychkin, I. Sashin, and A. Murani, J. Appl. Phys. **85**, 5344 (1999).
[38] T. Ebihara, Y. Inada, M. Murakawa, S. Uji, C. Terakura, T. Terashima, E. Yamamoto, Y. Haga, Y. Onuki, and H. Harima, J. Phys. Soc. Jpn. **69**, 895 (2000).
[39] H. Okamura, T. Ebihara, and T. Nanba, Acta Phys. Pol. B **24**, 1075 (2003).
[40] H. Okamura *et al.*, J. Phys. Soc. Jpn. **76**, 023703 (2007).
[41] T. Ebihara, E. D. Bauer, A. L. Cornelius, J. M. Lawrence, N. Harrison, J. D. Thompson, J. Sarrao, M. F. Hundley, and S. Uji, Phys. Rev. Lett. **90**, 166404 (2003).
[42] S. Burdin and P. Fulde, Phys. Rev. B **76**, 104425 (2007).
[43] J. L. Sarrao, C. D. Immer, C. L. Benton, Z. Fisk, J. M. Lawrence, D. Mandrus, and J. D. Thompson, Phys. Rev. B **54**, 12207 (1996).
[44] E. Figueroa, J. M. Lawrence, J. Sarrao, Z. Fisk, M. F. Hundley, and J. D. Thompson, Solid State Commun. **106**, 347 (1998).

[45] K. Takegahara and T. Kasuya, J. Phys. Soc. Jpn. **59**, 3299 (1990).
[46] K. Behnia, D. Jaccard, and J. Flouquet, J. Phys.: Condens. Matter **16**, 5187 (2004).
[47] C. Dallera, M. Grioni, A. Shukla, G. Vankó, J. L. Sarrao, J. P. Rueff, and D. L. Cox, Phys. Rev. Lett. **88**, 196403 (2002).
[48] S. R. Garner, J. Hancock, Y. Rodriguez, Z. Schlesinger, B. Bucher, Z. Fisk, and J. L. Sarrao, Phys. Rev. B **62**, R4778 (2000).
[49] M. Očko and J. L. Sarrao, Physica B **312-313**, 341 (2002).
[50] T. Mito, T. Koyama, M. Shimoide, S. Wada, T. Muramatsu, T. C. Kobayashi, and J. L. Sarrao, Phys. Rev. B **67**, 224409 (2003).
[51] A. Mitsuda, T. Ikeno, Y. Nakanuma, T. Kuwai, Y. Isikawa, W. Zhang, and Y. Yosimura, J. Magn. Magn. Mater. **272-276**, 56 (2004).
[52] T. Park, V. A. Sidorov, J. L. Sarrao, and J. D. Thompson, Phys. Rev. Lett. **96**, 046405 (2006).
[53] T. Mito, M. Nakamura, M. Otani, T. Koyama, S. Wada, M. Ishizuka, M. K. Forthaus, R. Lengsdorf, M. M. Abd-Elmeguid, and J. L. Sarrao, Phys. Rev. B **75**, 134401 (2007).
[54] I. Aviani and M. Ocko (unpublished).
[55] A. Severing, E. Gratz, B. D. Rainford, and K. Yoshimura, Physica B **163**, 409 (1990).
[56] W. Zhang, N. Sato, K. Yoshimura, A. Mitsuda, T. Goto, and K. Kosuge, Phys. Rev. B **66**, 024112 (2002).
[57] J. K. Freericks and V. Zlatić, Phys. Rev. B **58**, 322 (1998).
[58] J. K. Freericks and V. Zlatić, Rev. Mod. Phys. **75**, 1333 (2003).
[59] M. O. Dzero, L. Gor'kov, and A. K. Zvezdin, J. Phys.: Condens. Matter **12**, L711 (2000).
[60] M. O. Dzero, J. Phys.: Condens. Matter **14**, 631 (2002).
[61] T. C. Kobayashi *et al.*, J. Phys.: Condens. Matter **19**, 125205 (2007).
[62] M. C. Bennett, P. Khalifah, D. A. Sokolov, W. J. Gannon, Y. Yiu, M. S. Kim, C. Henderson, and M. C. Aronson, arXiv:0806.1943 (unpublished).
[63] A. T. Holmes, D. Jaccard, and K. Miyake, Phys. Rev. B **69**, 024508 (2004).
[64] D. Jaccard, H. Wilhelm, K. Alami-Yadri, and E. Vargoz, Physica B **259-261**, 1 (1999).
[65] H. Wilhelm and D. Jaccard, Phys. Rev. B **66**, 064428 (2002).